COVALENT LAYER-BY-LAYER SYNTHESIS OF RESPONSIVE POROUS FILTERS

A Thesis

by

AINSLEY LARUE ALLEN

Submitted to the Office of Graduate Studies of
Texas A&M University
in partial fulfillment of the requirements for the degree of

MASTER OF SCIENCE

May 2011

Major Subject: Chemistry

Covalent Layer-by-Layer Synthesis of Responsive Porous Filters

COVALENT LAYER-BY-LAYER SYNTHESIS OF RESPONSIVE POROUS FILTERS

A Thesis

by

AINSLEY LARUE ALLEN

Submitted to the Office of Graduate Studies of
Texas A&M University
in partial fulfillment of the requirements for the degree of

MASTER OF SCIENCE

Approved by:

Co-Chairs of Committee,	James D. Batteas
	David E. Bergbreiter
Committee Members,	Melissa A. Grunlan
	Karen L. Wooley
Head of Department,	David H. Russell

May 2011

Major Subject: Chemistry

ABSTRACT

Covalent Layer-by-Layer Synthesis of Responsive Porous Filters. (May 2011)

Ainsley LaRue Allen, B.S., United States Air Force Academy

Co-Chairs of Advisory Committee: Dr. James D. Batteas
Dr. David E. Bergbreiter

Poly(*N*-isopropylacrylamide) (PNIPAM), a temperature responsive polymer, undergoes a phase change at a lower critical solution temperature (LCST) in aqueous solutions. For PNIPAM this temperature is 32 °C in water. Below the LCST, the polymer is readily solvated by water. As the temperature of the solution increases, the polymer undergoes a phase transition so that above the LCST it is no longer water soluble. The LCST of PNIPAM may be changed by the addition of salt solutions from the Hofmeister series which will follow the Hofmeister effect for salting-in and salting-out the polymer.

Temperature responsive polymers may be grafted to a surface in a variety of methods to create responsive thin films that exhibit a change in wettability. The surface wettability is directly related to the polymers ability to be solvated in its coil conformation. When PNIPAM is grafted to a surface, the surface becomes alternatively hydrophobic and hydrophilic in response to both temperature and the anions in the Hofmeister series which take the surface either above or below the LCST of PNIPAM.

The synthesis of responsive nanocomposite grafts was successfully applied to glass slides and three-dimensional surfaces, porous glass frits which were capable of controlling

the passive flow rate. The nanocomposite graft was assembled in a covalent layer-by-layer approach to create more chemically robust surfaces, and also to incorporate nanoparticles into the graft for increased surface roughness and therefore improve wettability response. Because of a much greater inherent roughness to a glass frit, characterization of the polymers and nanoparticles was performed before they were covalently bound to the surface. The final product, a functionalized frit with a PNIPAM/SiO_2 nanocomposite graft, was analyzed by observing changes in the passive permeation rate of the frit between water and salt solutions. These changes in flow were indicative of the surface bound PNIPAM changing between its hydrophilic and hydrophobic conformation in response to water and concentrations of kosmotropic salts such as sodium sulfate and sodium citrate. In addition to the solute response, the frit was also determined to be responsive to temperature and concentration. Water exhibited a passive flow rate 1000 times faster than a kosmotropic salt but had a similar flow rate to that a chaotropic salt. By measuring the flow rate of 0.5 M Na_2SO_4 at ~7 °C in a cold room and at room temperature it was observed that sodium sulfate in the cold room passed through the frit at a rate 100 times faster than at room temperature. Because of the hysteresis of PNIPAM documented in literature, washing procedures were kept consistent between experiments to achieve more reproducible results.

It was concluded that the frits were temperature responsive and had relative standard deviations below 25 % for flow rates on a single frit. However, standard deviations of flow rates between frits were higher. This was likely due to a combination of factors, such as the frits' pore size range of 10 μm resulting in the possibility of varied degrees of functionalization of each frit.

DEDICATION

I would like to dedicate this thesis to my family and friends who have all been so supportive.

ACKNOWLEDGEMENTS

I would like to thank my committee chairs, Dr. Bergbreiter and Dr. Batteas, for their guidance and patience particularly in all academic and research aspects, but also in administrative aspects. I would also like to thank Dr. Wooley and Dr. Grunlan for serving on my advisory committee.

Thanks also to my friends, colleagues, and the department faculty and staff for making my time at Texas A&M University a great experience. And finally, thanks to my mother and father, my aunts and uncles, and my Mimi, for their unwavering support and love.

Thanks to the Air Force for allowing me the time to finish my research. The views expressed in this thesis are those of the author and do not necessarily reflect the official policy or position of the Air Force, the Department of Defense or the U.S. Government.

TABLE OF CONTENTS

CHAPTER Page

LIST OF SCHEMES

LIST OF FIGURES

FIGURE Page

LIST OF TABLES

CHAPTER I

INTRODUCTION

The use of synthetic processes to modify polymers has been important since the vulcanization of natural rubber in the early 1840s, which was closely followed by the manufacture and use of celluloid. At the turn of the 20th century, the first fully synthetic polymer, Bakelite, was synthesized and applied in a wide range of fields from the electrical industry, to toy cars, to the first plastic radios.[1] Today, several researchers are working to apply stimuli-responsive polymers, or "smart" polymers, to a comparable broad spectrum of applications, especially in the fields of medicine, microfluidics and surface chemistry. Because of their current and potential applications in a wide variety of fields such as biomaterials,[2] microfluidics,[3] surface wettability,[4] and drug delivery,[5,6] stimuli-responsive polymers are a major focus of chemical research.

"Smart" polymers respond to stimuli such as temperature, solvent, pH, electric fields, and mechanical stress that induce a useful change in the polymer's physical properties. Temperature responsive polymers make up the vast majority of smart polymers. These temperature responsive materials have tunable responsive behavior changes in response to changes in solvent,[7] polymer chain size,[8] or pressure.[9] One of the most common temperature responsive polymers is poly(*N*-isopropylacrylamide) (PNIPAM). Aqueous solutions of PNIPAM, poly(vinyl methyl ether) and poly(propylene glycol), along with polymers such as

---

This thesis follows the style of the *Journal of the American Chemical Society*.

polystyrene in methyl acetate,[9] polyisobutylene in ethane,[10] polydimethylsiloxane in butane,[10] are considered temperature responsive polymers because they have a lower critical solution temperature (LCST). An LCST is the temperature at which a polymer exhibits a phase change such that the polymer is no longer soluble. When the polymer is solvated, it maintains a spread out coil conformation; however, as the temperature of the solution increases the polymer changes to a globule conformation and comes out of solution (Figure 1).

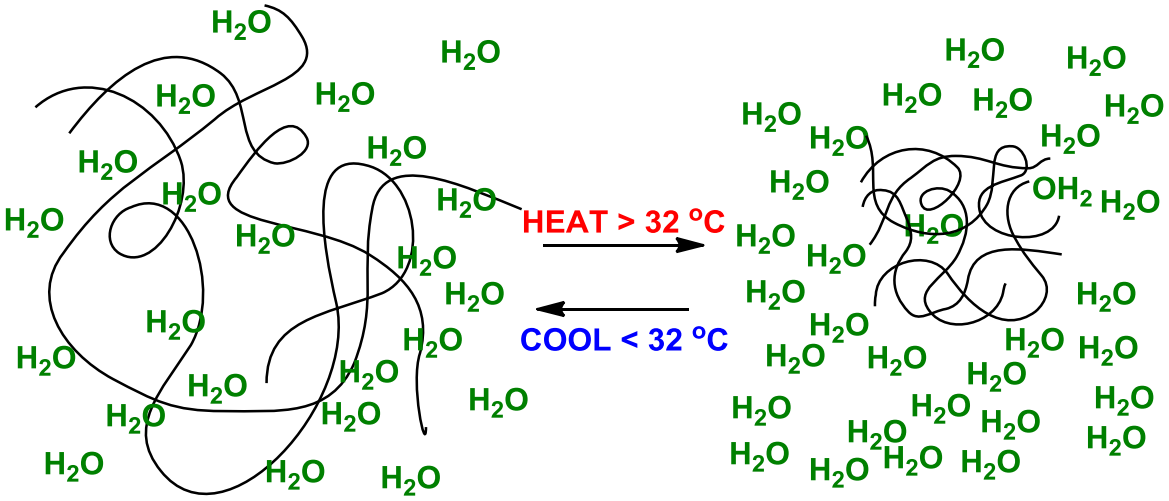

Figure 1. Phase transition of PNIPAM above and below the LCST.

Although polymers can exhibit LCST behavior in non-aqueous solutions, the remainder of this discussion will focus on the LCST of polymers in aqueous solutions since LCSTs in water are most relevant to the research described in this thesis.

The LCST effect in an aqueous solution can be described in an oversimplified but useful way using the Gibbs equation and the contributions of enthalpy and entropy to a

favorable negative ΔG. In this description of aqueous systems exhibiting the LCST phenomenon, dissolution occurs because each polymer contains hydrophilic groups that are solvated due to hydrogen bonding between those groups and the water molecules. This solvation provides an enthalpic advantage for the system. However, the necessary ordering of water molecules results in a less favorable ΔS and creates an unfavorable change in the entropy of the solution.[11] As the temperature is increased, the overall value of ΔG becomes increasingly less negative because of the importance of the entropic term of the Gibbs equation.

$$\Delta G = \Delta H - T\Delta S$$

At some critical temperature, the ΔH and "-TΔS" terms become equal and any further temperature increase leads to an unfavorable positive ΔG. Thus, the polymer solubility changes to create a favorable positive ΔS and the solvated coil conformation, present at low temperature, becomes desolvated leading to visually phase separated material (as ΔG remains negative) via a globular conformation.[11]

PNIPAM is particularly important in the field of stimuli responsive polymers. It has a lower critical solution temperature of 32 °C which lies between room temperature and body temperature and therefore allows for several biomedical applications such as drug delivery.[12] This phase transition and change in solubility has been used to release drugs.[6,13,14] When the temperature is raised above the LCST, the polymer undergoes a phase change causing a switch from a hydrophilic to a hydrophobic conformation. PNIPAM and other polymers having an LCST are shown in Scheme 1. PNIPAM has both hydrophobic alkane groups and hydrophilic amide groups that allow for favorable solvation in the coil conformation and

unfavorable in the globular conformation at higher solution temperatures. Several *N*-alkyl poly(acrylamides) exhibit LCST behavior at a wide range of temperatures. Poly(*N*-ethyl-*N*-methylacrylamide), a structural isomer of PNIPAM, has an LCST of 74 °C.[15] Changing the substituent on the nitrogen may have a small or large effect of the LCST. Poly(diethylacrylamide) and poly(*N*-cyclopropylacrylamide) have LCSTs of 30 °C and 53 °C respectively.[14, 16] Other polymers with LCSTs and little structural relationship to PNIPAM include poly(vinyl methyl ether) at 37 °C, and polyethylene oxide (PEO) ranging from 100 °C to 180 °C depending on the molecular weight.[17] These polymers and their LCSTs are shown in Scheme 1.

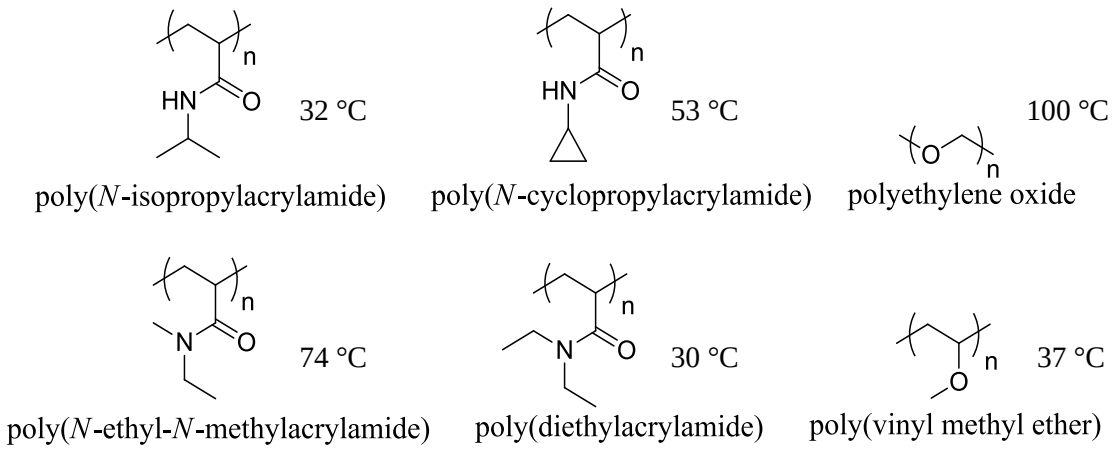

Scheme 1. Polymers with LCSTs.

The LCST of a polymer can be measured with several techniques such as light scattering, atomic force microscopy (AFM), ultraviolet-visible spectroscopy (UV-Vis) or fluorescent dye labeling. A newer technique developed by our lab uses a melting point

apparatus to measure the clouding curve of a polymer solution as a function of temperature.[18] When a temperature responsive polymer is in solution and is taken from below the LCST to above the LCST, the polymer phase separates from solution. The resulting polymer phase causes the solution to become cloudy. By measuring the light scattering as a function of temperature, an LCST can be measured. Typically the LCST is defined as the temperature at which light scattering is first observed. LCSTs can be determined via a number of light scattering techniques. The data for PNIPAM shows a relatively narrow phase transition which was first observed by Kubota using dynamic laser light scattering.[19] Wu and coworkers observed the phase transition at 32 °C for PNIPAM using both static and dynamic laser light scattering.[20,] Laser light scattering has also been used to determine the extent of swelling for the transition of a PNIPAM hydrogel.[21] The information about the narrow LCST gives crucial data needed for biomedical applications, particularly tissue engineering.[22] However, one of the main disadvantages is that light scattering techniques have been time consuming; the research groups of Bergbreiter and Cremer, developed a high throughput technique, in which clouding data was detected as a function of position rather than time.[14] Capillary tubes filled with PNIPAM solution were placed in a temperature gradient across the LCST so that by using dark field microscopy, the LCST could be determined by the distance at which the solution started to scatter light.[14] This method allowed differentiation between LCSTs that are within 1 °C of one another without requiring a narrow polydispersity.[14] Differential scanning calorimetry (DSC) is also capable of determining an LCST by measuring the temperature of the endothermic peak observed when the polymer precipitates out of solution.[23] This method is significantly more time consuming than

measuring scattering along a temperature gradient or using a melting point apparatus. Ultraviolet-visible (UV) spectroscopy may be used to measure the decrease in transmittance over a changing temperature gradient.[24] Unfortunately, this method requires a relatively large amount of polymer sample to be effective. For convenient detection, an automated melting point apparatus is a common tool that may also be used to measure LCSTs. When using the melting point apparatus, the increase in clouding, due to the phase separation of PNIPAM, increases the scattering intensity over an increasing temperature to yield a sigmoidal curve. Typically, the LCST is recorded at 10% scattering to avoid any convolution of the data at the baseline.

Extensive research has been done and continues to be done to determine the mechanism of the coil to globule transition observed at the LCST. Several of the techniques used to measure the LCST are also employed to determine how and why the transition occurs. For example, Wu and coworkers used static and dynamic laser light scattering to determine that the phase transition of PNIPAM actually had 4 distinct phase transitions.[25,26] These transitions were based on the hysteresis of the polymer by measuring the radius of gyration as a function of temperature.[26] By comparing the radius of gyration to the hydrodynamic radius, the polymer was determined to have thermodynamically stable coil, crumpled coil, molten globule, and globule conformations.[26] Polymer-dye interactions have also been examined in order to investigate the PNIPAM phase transition; the florescent dyes have supported the coil to globular transition theory.[13] Kolaric and coworkers saw a bathochromic shift in the fluorescence wavelength when PNIPAM with the fluorescent cyanine dye was heated from 30 °C to 32.5 °C. They concluded the shift was due to an

increase in the polarizable environment as the polymer chains revert to a globular conformation replacing water molecules around the first solvation sphere of the dye.[13] Fourier-transform infrared spectroscopy (FTIR) has been used to determine that both the hydrophobic and hydrophilic portions of PNIPAM are involved in the phase transition in the presence of water as well as in mixtures methanol and water.[7] Other experimental tests of PNIPAM in solution include viscosity measurements[27] or NMR.[28]

Several factors are known to affect the LCST of thermoresponsive polymers. Creating a copolymer is one of the most common ways to modify the LCST. The incorporation of hydrophilic groups or hydrophobic groups on the backbone is an easy way to bring an LCST close to a desired value.[29, 30] Hydrophilic groups tend to lower the Gibbs free energy for solvating the polymer and therefore increase the temperature at which the solvation process is no longer favorable.

External effects of the solution are also known to change the LCST. A prime example is the effect of salts on a polymer solution, where the aqueous environment around the polymer is maintained. The Hofmeister series, originally discovered in 1888, is based on an ion's ability to salt-out proteins in aqueous solutions.[31] The typical order of the Hofmeister anion series is as follows:

$$CO_3^{2-} > SO_4^{2-} > H_2PO_4^- > F^- > Cl^- > Br^- \approx NO_3^- > I^- > ClO_4^- > SCN^-.$$

The anions to the left of Cl^- are typically considered kosmotropes and possess a salting-out effect for proteins. The anions to the right of Cl^-, called chaotropes, lead to a salting-in of proteins. Polymers such as PNIPAM model the effect of cold denaturation of proteins in the presence of kosmotropic salts due to the presence of its hydrophobic and

hydrophilic groups.[32] The terms kosmotrope and chaotrope originated from the idea that these anions were capable of making or breaking water structure respectively.[32] However, it has been recently postulated that the ion interaction with the polymer (or protein) has a greater effect on the solubility of the polymer.[32]

Using dark field microscopy to measure LCSTs as a function of position, Zhang and coworkers determined details of the mechanism by which the Hofmeister series of anions affects the phase transition.[32] The kosmotropic salts lead to a salting-out effect of PNIPAM which causes the polymer to desolvate. As shown in Figure 2(b) below the anions interact with the hydrophobic polymer backbone and isopropyl groups resulting in an increase in surface tension.[32] Increasing the surface tension makes it more difficult for water molecules to hydrophobicly hydrate the alkane chains.[33] Additionally, the anions are able to polarize the water molecules responsible for hydrating the amide group though hydrogen bonding (Figure 2(a)).[32] The interaction between the ion and water weakens the hydrogen bond between the water and the amide moiety, leading to precipitation of the polymer.[32] However, chaotropic ions have been found to lead to a salting-in effect allowing the polymer to remain in solution.[32] This salting-in is due to the interaction of chaotropic anions with the amide group to help increase solubility, as depicted in Figure 2(c). Although there is a competing mechanism of increasing surface tension for the hydrophobic portions of the molecule, the anion polymer interaction allows the polymer to remain in solution.[33]

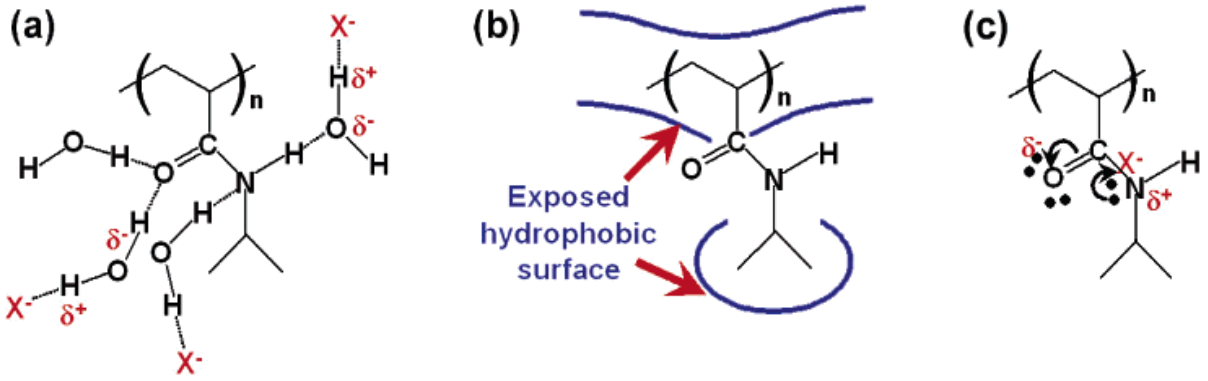

Figure 2. Effects of Hofmeister anions on PNIPAM solvation. (a) Anionic binding to water molecules weakens the hydrogen bonding to the hydrophilic amide group. (b) The anions increase the surface tension of hydrophobic regions thereby decreasing the hydrophobic hydration of the polymer. (c) Anions can also bind directly to the amide group. [Reprinted with permission from ref 32. Copyright 2005 American Chemical Society.]

Salt effects on the solubility of PNIPAM were found to be concentration dependent.[32] The change in LCST as a function of salt concentration for the Hofmeister series is shown in Figure 3. The extent of these salt effects is highlighted in the case of sodium carbonate where the LCST of PNIPAM was lowered to 21 °C for a concentration of only 0.3 M Na_2CO_3. However, chaotropic salts, such as NaSCN, lead to less significant changes in the LCST with increasing salt concentrations.

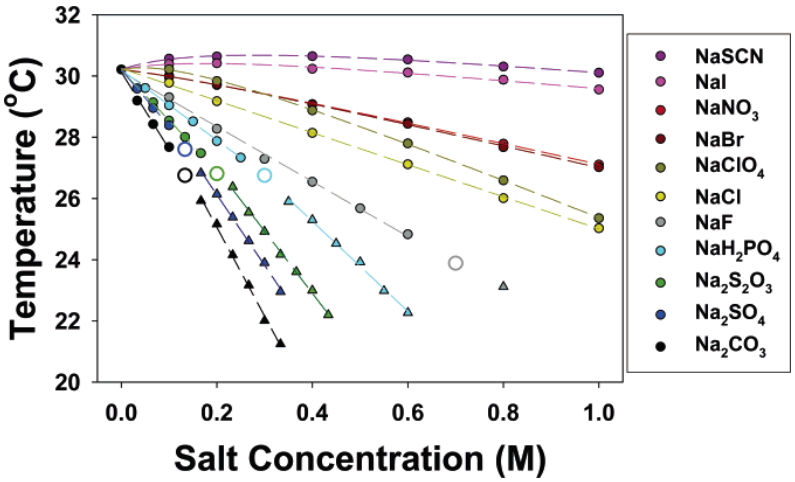

Figure 3. Effect of Hofmeister anions on the LCST of PNIPAM at increasing concentrations. [Reprinted with permission from ref 32. Copyright 2005 American Chemical Society.]

The open circles in Figure 3 for the five kosmotropic salts, namely sodium carbonate, sodium sulfate, sodium thiosulfate, sodium dihydrogen phosphate, and sodium fluoride, represent the concentration after which two separate steps for the phase transition are observed by measuring the scattering as a function of position over a temperature gradient.[32] After this data point, the graph shows the lower of the two transition temperatures. By using this method, the research groups of Zhang and coworkers were able to infer distinct information about the phase transition mechanism.[32] The first phase transition was found to be congruent with the dehydration of the amide and the second with dehydration of the hydrophobic portion of the polymer as seen in Figure 2(a,b).[32] Additionally, the chaotropic salts show a non-linear dependence on salt concentration.[32] Increasing temperature changed the LCST by changing the amount of time that it took for the anion to bind to the amide group and facilitate the salting-in effect as seen in Figure 2(c) in competition with the salting-out effect of increasing surface tension.[33]

There are potentially numerous applications for temperature responsive polymers and their tunable LCSTs. As mentioned earlier, biomedical applications are probably the fastest growing area of research for these polymers. Primarily, researchers are investigating methods to deliver drugs, enzymes, and genes,[34] as well as assist gene engineering,[35] and aid tissue growth in tissue engineering.[36,37] In order to gain strict control of polymer LCSTs for biomedical applications, researchers control molecular weight and combine the thermosensitive polymer with other useful functional groups.[37,38] When combined with other functional groups, on use of copolymers is to form micelles such that the outer shell is composed of the hydrophilic groups and the inner core contains the hydrophobic groups.[38] Encapsulating polymers such as PNIPAM-*c*-poly(methyl methacrylate) open the door for exploring the use of biomaterials, such as many lipophilic drugs, previously abandoned due to their low aqueous solubility (an important property for biomaterials).[38] The drugs may be incorporated as guest molecules into the hydrophobic center so that when the micelle undergoes a phase change, triggered by an external stimuli, the guest molecules are squeezed out of the micelle or allow the micelle to fall apart; both release the enclosed cargo.[5,39] The LCST of some of these micelles may be further fine-tuned by the interaction of copolymer functional groups with the guest molecule.[40] For example, using a PNIPAM-acrylic acid copolymer increases the uptake of dopamine that can then be used for drug delivery.[41] This is due to the anionic properties of the copolymer below pH 6.5 which could favorably interact with the cationic dopamine.[41]

In order to further control drug release or the release of other encapsulated molecules, temperature responsive micelles and hydrogels may be cross-linked.[2, 6, 42-44] Adding

crosslinks allows the structural integrity of the micelle to remain intact when the polymer phase change causes swelling and de-swelling in response to external stimuli which allows for the release of encapsulated guest molecules.[45]

The application of grafting responsive polymers onto a surface is the main focus this thesis.[30,31] By utilizing these materials on surfaces, different applications of responsive polymers can be investigated which were previously limited to solution state properties. Responsive surface applications include manipulating liquids by controlling flow rates,[3, 12] chemical sensing of the environment as indicated by a phase change,[46,47] biocompatibility of amphiphilic polymers,[48] and drug release from carefully synthesized micelles which disassemble in response to a stimulus.[49,50] Additionally, thermoresponsive polymers may be used to make alternatively hydrophobic and hydrophilic surfaces in response to external stimuli.[51,52] When anchored to surfaces and in the presence of solution, the polymers undergo the same phase transition as they would in solution except that there are one or more bonds to a surface. Therefore, when the responsive polymer is in its hydrophobic conformation above the LCST, the surface becomes hydrophobic which is proven by a change in the measured contact angle.[53]

Responsive surfaces may refer to the surface of hydrogels,[54] self-assembled monolayers,[55,56] or covalently grafted polymers.[35,57-59] Polymer coated surfaces may be applied to many materials, including metals, silicon, and plastics. This thesis focuses on covalent layer-by-layer (LbL) assembly of thermoresponsive polymers on glass surfaces. The application of LbL assembly has been used since the development of lacquerware by the ancient Chinese during the Qin Dynasty.[60,61] However, in recent history, the LbL assembly

has been mainly oriented towards building surfaces through hydrogen bonding[62,63] or inoic bonding.[64] Lacquerware on the other hand is the first example known to scientists of a covalent LbL assembly process.[60] It is a simple process of applying sap from lacquer trees many times over. During the drying process, the phenolic lipids from the sap undergo polymerization to create the glossy finish.[60] In order for LbL assembly to be effective, several conditions must be met. First, the polymers and materials being used must have functional groups that are capable of forming the covalent bonds.[60] If a polymer does not or cannot be modified to include such functional groups there will be no way to apply this building process. Second, for these surfaces to have good applications they must be easily separated from any side products formed in the reaction.[60] Well controlled surfaces are imperative not only for accurate research, but also for when they are used in drug delivery or to assist tissue engineering.[50] Third, in order to make these surfaces with relative ease the reactions for the LbL assembly should be feasible in ambient atmosphere and may be carried out in aqueous or organic solvents.[60] Covalently assembled surfaces afford advantages over ionic or hydrogen bonded surfaces in that they are more robust and will not dissemble simply under high pH or ionic strength.[60] By using covalent bonds to build responsive surfaces, a wide range of surfaces could be obtained by including a number of different functional groups.[60] Such and coworkers used azide and alkyne functional groups to create a cross linked layer-by-layer assembly of poly(acrylic acid).[65] Click chemistry was used for this surface to form covalent crosslinks because of its high yields under mild conditions, allowing for facile synthesis of robust covalently bound polymers.[65]

The LbL assembly process is one way to build these robust surfaces, and it is commonly referred to as a "grafting to" method. To begin the LbL assembly, a nucleophilic surface should be exposed to an electrophilic solution (or an electrophilic surface exposed to a nucleophilic solution). The surface should then be allowed to react with an electrophilic solution completing the first layer. By alternatively exposing the surface to electrophilic solutions and nucleophilic solutions, the surface is built one monolayer at a time. In this method the responsive polymer is synthesized away from the surface and therefore may be characterized before binding to the surface.[66] Characterization methods apart from the surface, allow for better determination of the purity and functional groups of the polymer. Analytical methods such as infrared (IR) spectroscopy, nuclear magnetic resonance (NMR) spectroscopy, LCST determination, and melting point determination are all used. Because the functional groups which react with the surface are known, surface analysis techniques, such as contact angle measurements or AFM roughness measurements for grafted temperature responsive polymers, would provide a ready diagnostic to confirm the successful fabrication of the surface with responsive wettability.

Another method of covalent assembly is commonly known as "grafting from" the surface. This involves polymerization reactions taking place from initiators already grafted onto the surface. The "grafting from" method is most often used to form a polymer brush surface, one in which the polymers are end grafted and spread out from the surface in a brush-like fashion. However, when using the "grafting from" approach, polymer brushes can easily become overly dense.[66] If this is the case, phase changes of grafted responsive polymers from the coil to the globular conformation would be hindered by a lack of space.[66]

Without the physical transition, the effects such as changing from a hydrophilic surface to a hydrophobic surface will not be observed. Thus the "grafting from" method contains some limitations for synthesizing polymer brushes to make responsive surfaces.

The simplest method of synthesizing these polymers from the surface is controlled radical polymerization, because of its applicability to a wide variety of functional monomers.[66,67] The surface is activated by starting the surface growth using monomers that contain radical initiators.[67] Atom transfer radical polymerization (ATRP) as a means of controlled polymerization from a surface, yields surfaces of end grafted polymers with relatively narrow polydispersities.[67] Because of the ease of initiator formation and simple polymerization conditions, ATRP is one of the preferred controlled radical growth mechanisms.[68] To confirm the control offered by ATRP, ellipsometry can be used to measure the thickness of growing surfaces. Polymerization control is verified when linear increases in thickness are observed.[67] The addition of a Cu^{II} ligand provides a similar effect to the free initiators by serving as a deactivator while maintaining controlled growth.[67,68] For surface initiated polymerizations using ATRP, the polymer brush thickness has been determined to be related to M_n for polymers synthesized in solution. As such, the height of end grafted polymers can be estimated.[67] However, because of surface constraints, calculations to determine the polymer brush thickness are consistently longer than the ellipsometric measured thickness. This is because geometric constraints drastically slow the propigation for tethered polymers compared to polymers in solution.[67] Although the polymer heights were less than calculated, ATRP is still capable of growing relatively thick films in short periods of time. When water accelerated or aqueous ATRP is introduced, films as thick

as 700 nm have been manufactured in only 12 h compared to similar films of 100 nm thickness synthesized over 20 h.[67]

Surface initiated polymer growth also includes ring opening metathesis polymerization or ROMP. Although this method proves excellent for norborenes containing monomers, it has not been broadly applied because of the limited number of monomers cable of undergoing this reaction to create good brush thickness.[67, 68] Despite its limited reaction scope, the conductive coatings formed by these materials have well-defined brushes that have potential application in electronic devices.[67, 68] Ring opening polymerization (ROP) can also be used for polymer growth. Unlike ATRP, ROP may produce as little as 9 nm in polymer brush thickness even after seven days and therefore must be catalyzed with a free initiator such as benzyl alcohol to achieve thicker layers.[67] Other growth mechanisms include living anionic and cationic polymerizations. Jordan and coworkers created the first surface initiated anionic polymerization of styrene.[69] The reaction was performed using self-assembled monolayers on gold surfaces and was carried out under inert atmosphere conditions.[69] Because all cationic and anionic assemblies are very sensitive to reaction conditions, little work has been carried out using these methods.

Grafting polymers onto particles is a rapidly growing application for polymer growth on surfaces which yields "hairy particles."[70] One of the most common methods of particle functionalization is the use of two or more polymer brushers. Due to their tunability and attractive potential applications, silica nanoparticles were functionalized by Zhao and coworkers using a mixture of poly(tert-butyl acrylate) (PtBA)/polystyrene (PS) brushes by sequential ATRP.[70] These particles were beneficial in that they became the first

experimental study of the phase morphology of mixed polymer brushed on a curved surface. They also introduced apt synthetic precursors of poly(acrylic acid)/PS functionalized particle surfaces which were responsive to their solvent environment.[70] Other functionalized curved surfaces have been developed and also have applications in technological fields, biomedical fields, catalysis, and surface wettability.[70]

Other synthetic schemes for polymeric responsive surfaces form covalent bonds by crosslinking the material after it is spin coated onto the surface.[71] This method usually involves creating a copolymer of the desired responsive polymer with new substituents capable of crosslinking to one another. Iwata and coworkers prepared PNIPAM-*c*-MOIBM (2-(0-(10-methylpropylideneamino) carboxyamino) ethyl methacrylate), which upon heating the isocyanate group is deprotected and capable of coupling to form urethane bonds.[71] Other surfaces which utilize crosslinks include hydrogels. Hydrogels are polymeric networks, formed by crosslinking polymers, that are capable of swelling and de-swelling while still maintaining their general shape.[2] Gil and coworkers developed a network of PNIPAM and silk hydrogels by polymerizing a NIPAM/silk protein solution in the presence of *N,N'*-methylenebis(acrylamide) and *N,N,N',N'*-tetramethylethylenediamine.[2] Upon freeze-drying, the silk was physically cross-linked to support the macro porous structure.[2] The silk-hydrogel synthesis founded a method of developing robust gels capable of deswelling up to 73 % of its original size when above its LCST in solution.[2] Adding silk to the films not only stabilized the pores, but it also strengthened the structure, an important property for structure application.[2]

A non-covalent bonding method for designing responsive surfaces is ionic layer-by-layer assembly. These films are formed by submerging a surface in an anionic polyelectrolyte followed by a cationic polyelectrolyte.[72] Repeating this process alternates the charge of the surface and builds a graft one layer at a time.[72] Some advantages of using ionic methods over covalent methods are the speed with which the reactions occur and cost effectiveness.[73] Ionic LbL assembly has also been explored for biomedical applications such as drug delivery where encapsulating micelles would dissemble above or below a specific pH. Hydrogen bonding is another method of grafting polymers to a surface in a layered fashion. These films are synthesized by the interaction of hydrogen bonding donors and acceptors with the surface. For example, hydrogen bonded layers can be assembled by simply exposing the molecules to solutions of varying ionic strengths or acidities.[74] Rubner and coworkers found that hydrogen bonding could also be used to form hydrophobic or self-cleaning surfaces when combined with 50 nm silica nanoparticles.[75] In their experiment, a glass surface was alternatively dipped into poly(allylamine hydrochloride) (PAH) at a pH of 7.5 or 8.5 and poly(acrylic acid) (PAA) at a pH of 3.5 with washing in between each cycle.[75] The nanoroughness of the thin film, along with the near microroughness of the nanoparticles, caused the surface to mimic the behavior of a lotus leaf.[75]

The research presented here focuses mainly on tuning the wettability of surfaces synthesized by covalent layer-by-layer assembly. The hulls of boats, several biomedical devices, car finishes, select clothing, and many plastics are surfaces which desire a certain amount of wettability and being able to control this wettability adds a new dimension to

research. Measuring the contact angle of water on surfaces is the most common way of determining its wettability. This is done by using Young's equation.

$$\gamma_{LV}\cos\theta = \gamma_{SV} - \gamma_{SL}$$

The γ terms account for the surface tension of the liquid vapor (LV) contact, solid vapor (SV) contact and solid liquid (SL) contact.[76] Theta (θ) is the calculated contact angle. The higher the contact angle the less interaction there is between the surface and the water droplet, implying a hydrophobic surface. Using redox-active polymers, several researchers have successfully switched the wettability of select surfaces.[53] For example, Sondag-Huethorst and coworkers obtained a contact angle change of 10°, from 49° to 50°, by applying a voltage to oxidize ferrocene groups on the surface.[53] Abbott and Whitesides were able to control the shape of a water droplet on SAMs of 15-(ferrocenlylcarbonyl)pentadecanthiol on gold surfaces.[77] Their maximum wettability change was a change in contact angle of 28°, from 71° to 43°, when electrical potential was increased from 0.3 V to 0.5 V.[53,77] However, the change in wettability was not an entirely reversible process due to the decomposition of the ferrocenium ion.[77] Keeping with the major interest for responsive materials in the biomedical realm, electrochemical control of redox polymers may allow DNA adsorption and desorption.[53] Hook and coworkers found that amine rich allylamine plasma polymer will also demonstrate DNA adsorption in the presence of a positive applied voltage and will desorb the DNA at negative voltages.[53] Photoswitching usually induces changes in wettability due to a *cis* to *trans* conformation change brought on by photostimuli.[53] Using poly(vinyl alcohol) with azobenzene side

chains, the area of the monolayer increases as the azobenzene side chains change from the *trans* to *cis* with exposure to UV light.[78]

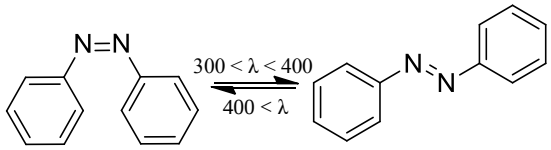

Scheme 2. *Cis* to *trans* conformational change of azobenzene due to exposure to UV light.

Photostimuli are often used to make a surface superhydrophilic. ZnO films for example were forced into an unstable conformation by irradiation with UV light to change the surface from superhydrophobic with a contact angle of 162° to superhydrophilic with a contact angle of 0°.[53] The wettability change was a temporary and reversible phenomenon.[53]

Environmental switching has been the longest studied stimuli response, but currently it is most researched for surfaces that have a combination of polymers which will respond differently to the same environment.[53] For example Zhao and coworkers synthesized poly(methyl methacrylate) (PMMA) and polystyrene (PS) brushes on a silicon wafer.[79] After treatment with cyclohexane, a solvent selective for PS, the surface had advancing contact angles of 84°; after treatment with glacial acetic acid, a solvent selective for PMMA, the surface roughness was increased thereby increasing the advancing contact angle to 92°.[79] These surfaces, have the advantage of being applicable to situations other than flat surfaces and responses other than surface wettability.[53] Liu and coworkers for instance synthesized a copolymer containing PAA and poly(butyl acrylate) to create polymer networks that respond to pH changes and have been demonstrated to successfully control the release of drugs.[53]

Mechanical stimuli have also been known to switch surfaces between hydrophilic and hydrophobic.[53] This transition is a simple effect of stretching out a polymer such as an elastic amide so that the water droplet will interact between the polymer chains when they are pulled apart.[53] The mechanical stress creates a hydrophilic surface, but when the applied stress is removed and the polymer conformation returns to its natural structure, which creates a hydrophobic surface.[53]

Studies on temperature responsive changes in wettability showed increases in contact angles as the surface is changed from hydrophilic to hydrophobic. For example, changes of about 30° were observed for PNIPAM brushes grafted onto a silicon surface using surface initiated polymerization.[53, 80] The surface is responsive for the same reason the polymer precipitates out of solution. When the solution and surface are above the LCST, the polymer is in its hydrophobic conformation and has poor interactions with water. Therefore, the surface becomes hydrophobic and the contact angle increases. Huber and others have utilized such PNIPAM functionalized surfaces in the fabrication of a microfluidics device that controlled the uptake and release of proteins such as myoglobin, bovine serum albumin, hemoglobin and a few others.[81] The proteins would interact with the PNIPAM surface above the LCST and be released at temperatures below the LCST.[53, 81]

Adding nanoparticles to temperature responsive surfaces to increase surface roughness and therefore wettability responsiveness is a relatively new area of responsive surfaces; it allows the surface to mimic hydrophobic properties found in nature such as on the lotus leaf. After synthesizing pure polymer surfaces, Sun and coworkers proceeded to make PNIPAM brush surfaces on rough silicon with groves ~ 6 μm apart. Below the LCST, water

on the PNIPAM surface had a contact angle of 0°.[80] At 40 °C the contact angle was increased to 149°.[80] Layer-by-layer assemblies using nanoparticles have also shown that as the overall roughness increases, the hydrophobicity of the functionalized surface increases.[57] Liao and coworkers incorporated functionalized silica nanoparticles into a PNIPAM graft and were able to obtain contact angle changes. In the same manner PNIPAM responds to temperature changes when grafted on the surface, it also responds to concentrations of anions in the Hofmeister series. Liao and coworkers used water and solutions of kosmotropic salts to obtain contact angle changes from 76° to 144°.[51] This proved surface grafted PNIPAM with silica nanoparticles capable of creating a solute responsive surface.[51]

The mechanical properties of these responsive surfaces have a significant effect on the experimental results. Looking strictly at PNIPAM grafted onto surfaces, the properties observed in solution differ slightly from those with one or more bonds to a surface. Results using surface plasmon resonance measurements and neutron reflectivity studies indicate that the phase transition of PNIPAM grafted to a surface occurs over a broad temperature range around 32 °C.[82] Quartz crystal microbalance is a popular technique for measuring the coil to globule transition of PNIPAM brushes.[72,82,83] Zhang and coworkers studied the frequency and dissipation of PNIPAM grafted onto a quartz crystal microbalance.[84] They found that the phase transition occurs in the range of 23 – 35 °C compared to the 30 – 32 °C for the phase transition in solution.[84] Additionally studies of the polymer returning to its original conformation revealed that a difference exists in the respective energies involved in the hydration and dehydration of PNIPAM.[84] In surfaces studied by Liu and coworkers, surface

grafted PNIPAM chains had not returned to their original "stretched out" conformation even after one week of cooling below the LCST.[83]

This thesis focuses on utilizing the specific properties of PNIPAM discussed above by incorporating PNIPAM into porous surfaces. Alem and coworkers used both free radical polymerization and ATRP to synthesize PNIPAM brushes on a track-etched poly(ethyleneterephthalate) (PET) membrane.[85] They found that the pore permeability for larger pores (330 nm) was more hindered by the hydrated chains occupying the pore space and was more permeable above the LCST when the chains were in the collapsed state. Smaller pores (80 nm) grafted with PNIPAM were able to control the rate of permeability of an electrolyte solution.[85] Below the LCST of PNIPAM the chains were highly hydrated and therefore lowered the permeation rate, but above the LCST, the PNIPAM chains in the collapsed state acted like a cork to the pores, preventing the electrolyte solution from coming in contact with or permeating the pores.[85] Peng and Cheg received similar results when grafting PNIPAM to porous polyethylene films.[86] At low grafting densities, vitamin B_{12} was able to permeate the membrane both above and below the LCST of PNIPAM; however, with a high grafting density, the polymer filled the pores and created a PNIPAM layer at the polyethylene-solution interface. Above the LCST this resulted in decreased permeation of the vitamin.

In the following chapters, the synthesis of PNIPAM-bound surfaces via covalent LbL assembly will be discussed, as well as the change in flow rates unique to these surfaces. PNIPAM/SiO_2 nanocomposite grafts were synthesized on glass slides and the same synthesis was applied to porous glass frits. These frits were treated with water and salt solutions from

the Hofmeister series and the passive flow rates slowed in response to kosmotropic salts compared to water. These changes were not only dependent on the solute identity but were also dependent on the concentration. The synthesis of the graft and the testing of reversibility of the responsive surface are discussed separately in the chapters that follow.

CHAPTER II

SYNTHESIS OF SURFACES WITH VARIABLE WETTABILITY IN RESPONSE TO SODIUM SULFATE

Introduction

Responsive surfaces are surfaces that respond to stimuli such as temperature, pH, electrical fields, ionic strength, or mechanical stress. These surfaces are of interest in many applications. For example, surfaces with responsive wettability have been used to prepare self-cleaning films, microfluidic devices, and to pattern cells on a surface.[87, 88] Responsive surfaces can be made using a variety of methods. The most common approach is to prepare polymer grafts at a surface by synthesis of polymer brushes that are initiated from the surface in a "grafting from" method. This grafting from method has been used by many groups and is illustrated by the work of Ober and coworkers who used this strategy to prepare pH-responsive polyacrylic acid grafts on gold.[89] An alternative approach to prepare a responsive surface is to attach a preformed polymer to the surface. This can be accomplished by using an appropriately terminally functionalized polymer or oligomer and a suitable surface. Berger and coworkers used this approach to synthesize Janus particles in which half of each silica particle was functionalized with carboxy-terminated poly(2-vinylpyridine) to prepare a second sort of pH responsive particle.[90] Finally, polymers can be grafted to surfaces by a polyvalent "grafting to" method using covalent, ionic or hydrogen bonds in a layer-by-layer (LbL) assembly process.[60]

Surfaces with responsive wettability may also be prepared from a surface that has a built in roughness by using free radical graft polymerization to modify the surface with polymer brushes. For example, Sun and coworkers started with silicon substrates, flat unmodified surfaces or surfaces that had been modified with a laser cutter to create microgrooves of varying spacing. They then grafted PNIPAM brushes on both surfaces using a surface grafted initiator to produce a responsive surface.[80] The flat silica PNIPAM-grafted surface exhibited a water contact angle change from 63° to 93° based on PNIPAM's temperature response when contact angles were measured at 25 and 40 °C respectively. By using an optimal groove spacing of 6 μm, the product PNIPAM-grafted surface had the necessary roughness to increase the contact angle that was measured above the LCST and the necessary capillary action to decrease the contact angle that was measured below the LCST. The total contact angle change on the rough surface was from 0° to 149° when contact angles of water were measured at 25 and 40 °C respectively.[80] Xia and coworkers proceeded to build on this method by synthesizing a bi-responsive surface that used a polymer that was pH and temperature responsive to make a PNIPAM-*c*-poly(acrylic acid) graft.[91] They combined the bi-responsive character of this polymer and enhanced surface roughness to synthesize a surface with highly controllable wettability that would respond to both temperature and pH. They showed that they could prepare a surface whose contact angle changed from 8° at 21 °C at a pH of 11 to a contact angle of 149° at 45 °C at a pH of 2.[91] They showed that this surface was bi-responsive by examining the wettability change at neutral pH.[91] The contact angle changed from 18° to 120° by only changing temperature from 21 °C to 45 °C. At a constant temperature of 25 °C the contact angle changed from 120° to 0° by changing only

the pH from 2 to 11.[91] Overall they could achieve a wettability change of 150° by starting at 25 °C and a pH of 11 and changing to a temperature of 45 °C at a pH of 2.

While the above approaches all afford surfaces with responsive wettability, our interests were to develop more conformal surface functionalization chemistry – chemistry that could be generally applied to both flat and three-dimensional surfaces. In this synthesis nanoparticles may be used to create rough surfaces within the 10 – 20 μm pores of a glass frit.[51] These particles have two functions – they serve to roughen the surface and are also functionalized so that the particle is a component of a LbL assembly process. These nanoparticles can either be designed such that they have a counter ion necessary for the electrostatic binding of an ionic LbL assembly or such that they contain a functional group necessary for formation of a covalent LbL assembly.[92] Incorporating nanoparticles when using the "grafting to" approach produces surfaces with increased hydrophobicity. This change in wettability can be assessed by measuring the contact angle and can be rationalized using Young's equation. Cassie and Baxter attributed the increased hydrophobicity of rough surfaces to trapped pockets of air within the surface.[93] To estimate the contact angle of a roughened heterogeneous surface that was composed of a solid substrate containing periodic void volumes, they concluded that the contact angle was dependent on a weighted combination of contact angles of the water in contact with the solid surface and air.[93] The contact angle of water on air is considered to be 180°.[93] The fraction of contact that the water droplet has with the surface and air is multiplied by the contact angle measured on that substrate to yield the following equation.[93]

$$\cos\theta_{12} = f_1\cos\theta_1 + f_2\cos\theta_2$$

Poly(*N*-isopropylacrylamide) (PNIPAM) is an ideal polymer for creating responsive surfaces. Its responsiveness stems from the fact that it has a lower critical solution temperature (LCST) of 32 °C. Above the LCST of PNIPAM, the polymer undergoes a phase transition such that it is no longer soluble in aqueous solutions. The phase transition occurs when the polymer chains' hydration decreases leading to a change from a highly solvated random coil to a less solvated tighter globular conformation. A simple interpretation of this transition attributes the change in solvation to the increase in the Gibbs free energy of the solvated polymer as the temperature increases. Hydration of PNIPAM in this argument is presumed to be favored enthalpically but disfavored entropically because of the requirement that solvation organized up to 3 water molecules per monomer unit. A higher temperature increases the importance of the positive $T\Delta S$ term and has little or no effect on the ΔH term. Thus, water hydration of PNIPAM is no longer favorable as temperature increases, and as the water is removed from the polymer, it becomes insoluble and adopts a hydrophobic conformation (Figure 1). The identical phenomena at a surface will lead to a surface changing from hydrophilic to hydrophobic as shown in Figure 4 and as is discussed below.

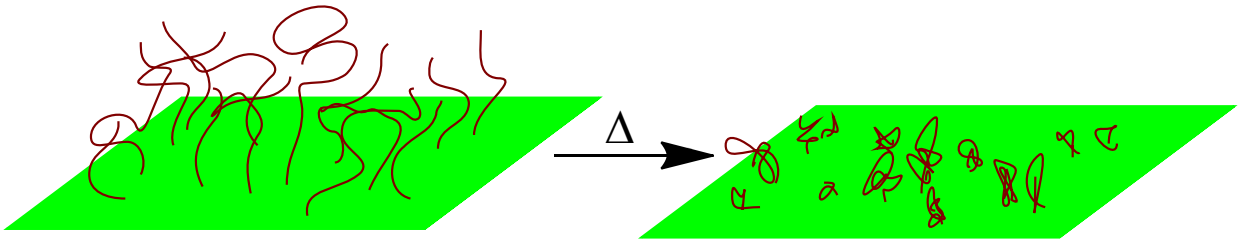

Figure 4. Structural phase change above and below the LCST of a PNIPAM on a surface.

In solution, the removal of water from the polymer chain means that PNIPAM is no longer soluble, and the solution becomes cloudy due to the formation of an insoluble PNIPAM phase. This process can be measured using a light scatting apparatus and was routinely measured when necessary in this work using a digital melting point apparatus. When PNIPAM is attached to the surface (as shown in Figure 4) and is in contact with aqueous solutions, the result of this same phase transition is that the surface becomes hydrophobic. This leads to the reversible hydrophobic/hydrophilic wettability properties of PNIPAM-grafted surfaces that can be measured with a contact angle goniometer.

In addition to temperature responsiveness, PNIPAM both in solution and on surfaces will also exhibit wettability that changes in response to the presence of various salts at various concentrations. Unlike the effects of surfaces modified with PNIPAM-*c*-PAA copolymers, this responsive wettability does not rely on a chemical reaction. Instead these changes in cloud point behavior or surface wettability are based on the fact that salts affect the LCST of PNIPAM. These effects are analogous to the Hofmeister effect on protein hydration and lead to changes in surface wettability in response to the concentration and identity of Hofmeister anions.[32, 33, 51] The greatest wettability response to Hofmeister anions was observed when the surface included a well-constructed nanostructure such that it was heterogeneous and rough.

This chapter discusses the synthesis of thin PNIPAM/SiO_2 films on glass substrates and the theory of how the structure of those surfaces enhances the wettability responsiveness. Nanocomposite PNIPAM/SiO_2 grafts were formed by a covalent layer-by-layer assembly first on functionalized PE films and then on glass surfaces. The PE film modification

replicated prior work in the Bergbreiter group.[51] The grafting of glass surfaces was designed to show that these functionalization procedures could be used on other surfaces and to determine if the solute sensitive reversible wettability seen with nanocomposite grafts on PE films was also observed on glass surfaces with similar nanocomposite grafts. Then the same process was used to functionalize medium porosity (10 – 20 μm pores) glass frits. The latter synthesis was designed to test if these synthetic procedures were indeed conformal and whether they could modify complex three-dimensional materials. The success of this procedure applied to porous glass frits was evaluated by experiments that probed the wettability of the surface which was expected to affect flow rates through the frit. These experiments where I evaluated the formation of a reversibly wet surfaces by observing the change in passive permeation of a solution through the frit above and below the LCST of PNIPAM are discussed in detail in Chapter III.

Synthesis of Starting Polymers and Materials Required for Preparing Responsive Glass/(PNIPAM/SiO_2)$_6$/PNIPAM Nanocomposite Thin Films

The covalent assembly process requires the use of pairs of reactive polyvalent reagents. In this synthesis we need electrophilic polymers and nucleophilic nanoparticles as components for the covalent reactions to build nanocomposite grafts on glass surfaces in a layer-by-layer assembly procedure. The electrophilic polymer used was either poly(*N*-acryloxysuccinimide) (PNASI) or a PNIPAM-*c*-PNASI copolymer. PNASI was synthesized using a free radical polymerization as shown in Scheme 3 and was characterized by nuclear magnetic resonance (NMR) and IR spectroscopy. In addition to the homopolymer PNASI, a

copolymer of PNIPAM-*c*-PNASI was also used in these syntheses as an electrophilic polyvalent reagent.

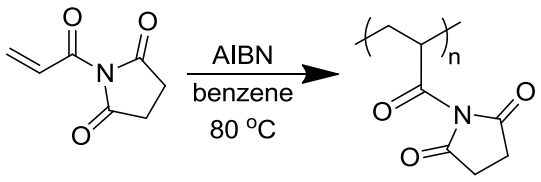

Scheme 3. Synthesis of PNASI by free radical polymerization.

This copolymer was synthesized by a free radical copolymerization (Scheme 4) and was characterized by NMR and IR spectroscopy. Integration of the peaks at 4.00 and 2.89 ppm due to the PNIPAM and PNASI groups respectively allowed us to determine that the two components, PNIPAM and PNASI, were present in a 9:1 molar ratio.

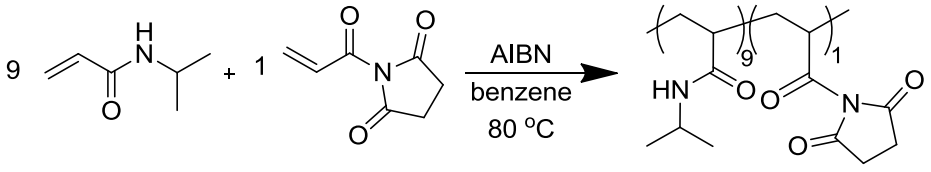

Scheme 4. Synthesis of PNIPAM-*c*-PNASI copolymer by free radical polymerization.

The polyvalent nucleophilic components of this layer-by-layer assembly process all contained polyamines. In the initial stages of this process, a glass surface was primed with polyamines as discussed below. In the layer-by-layer synthesis, the nucleophilic component was composed of 10- and 100-nm diameter silica nanoparticles that were functionalized

using 3-aminopropyltriethoxysilane (APTES) so that the surface of the particles would have multiple primary amine groups which can form amides with NASI groups of the PNIPAM-*c*-PNASI copolymer.

The nanoparticles used in this work were obtained from Sigma Aldrich and Fiber Optic Center Inc. and had to be functionalized with amines. Prior to functionalization the particles were thoroughly cleaned using a 5 % HCl solution. In the case of the 100-nm silica nanoparticles, the particle size and distribution was also measured. After cleaning, 100-nm silica particles were suspended in ethanol to create a dilute solution. This solution was drop cast onto a clean silicon wafer, and atomic force microscopy (AFM) was used to verify the size and determine the size distribution of the nanoparticles. The size distribution can be seen in the histogram below (Figure 5). A similar analysis has not been carried out on the 10-nm particles so the 10-nm particles however were labeled to have a size of 5 – 15 nm and were assumed to have a dispersity similar to that measured for the 100 nm particles.

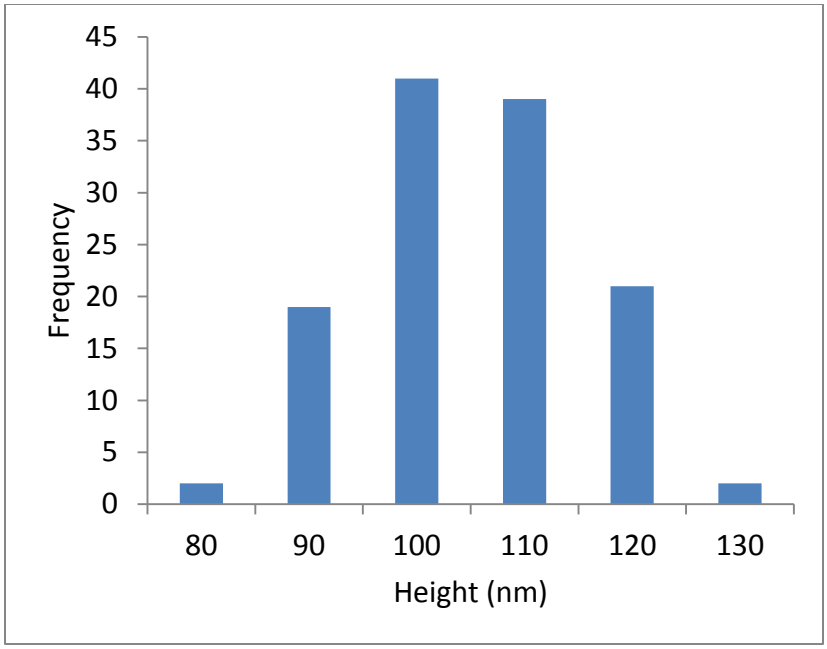

Figure 5. Particle size distribution of 100-nm silica nanoparticles as determined by AFM.

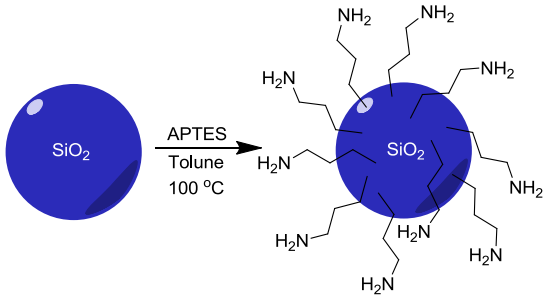

Scheme 5. Synthesis of aminated nanoparticles.

The nanoparticles were functionalized with APTES (Scheme 5). The loading of the surface bound amine groups was determined by treating 0.1 g of the aminated particles with an excess of HCl. An aliquot of the remaining HCl was titrated to a phenolphthalein end

point. The 10-nm particles had an amine loading with 0.67 mmol of $–NH_2$ groups / g of SiO_2 while the 100-nm had an amine loading of 0.24 mmol of $–NH_2$ groups / g of SiO_2.

Priming of Glass Surfaces in Preparation of Layer-by-Layer Assembly

Clean glass surfaces have contact angles near 0° and are completely hydrophilic. However, beginning the LbL assembly process with the surface hydroxyl groups was not expected to lead to enough grafting with PNASI or PNIPAM-*c*-PNASI copolymers. Thus, a glass slide was allowed to react with 3-aminoprypyltriethoxysilane (APTES) to form a more nucleophilic surface that would contain primary amines using the procedure shown in Scheme 6.[94] This synthesis includes a heating step to insure complete reaction of the triethoxysilyl groups with the surface hydroxyl groups. This APTES functionalization was carried out using the aqueous deposition method developed by Wang who previously reported that this method creates a surface more consistent with that of a monolayer than either vapor deposition, concentrated or dilute, or organic-phase deposition.[94]

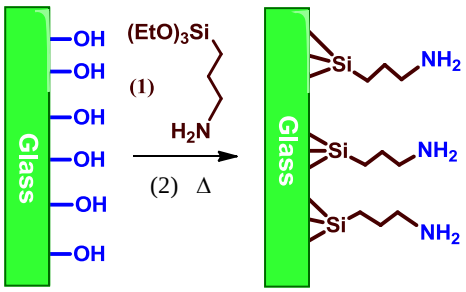

Scheme 6. Synthesis of an APTES layer on a glass slide.

While the schematic drawing of the surface in Scheme 6 suggests that a monolayer of APTES formed; amine groups have a high affinity for the glass surface and water catalyzes the binding of the silane molecules in a polymeric fashion. Thus, the formation of a multilayer surface of APTES may have occurred.[94, 95] This is of little consequence however for our chemistry. The success of the chemistry used in Scheme 6 to form an amino functionalized surface was tested by measuring the contact angle of the product of Scheme 5. The observation of an advancing water contact angle of around 40° versus the starting contact angle of 0° provided qualitative evidence for the success of this chemistry.

To minimize the number of steps needed to create the nanocomposite grafts we wanted to prepare, we carried out two other reactions to further increase the density and reactivity of these nucleophilic surfaces (shown in Scheme 7). These reactions involved formation of a more aminated surface using first poly(*N*-acryloxysuccinimide) (PNASI) treatment followed by polyethyleneimine treatment. In these steps, PNASI forms some amides with the amino groups at the surface, but surface constraints on these reactions leave multiple electrophilic active ester sites unreacted. Polyethyleneimine was then used to attack these unreacted ester sites to further increase the concentration of amines on the surface. The reaction of active esters with amines can be easily carried out at room temperature and the side product, *N*-hydroxysuccinimide (NHS), is easily washed away. Any of PNASI's NHS active ester groups that remain unreacted after PEI treatment were quenched with isopropylamine to form *N*-isopropylacrylamido groups. Two layers of PNASI/PEI quenched with isopropylamine were bound to the glass surface in this way to yield a surface with a denser array of nucleophilic amines for subsequent LbL assembly of a PNIPAM/SiO_2

nanocomposite. The success of these steps is evidenced by our ability to form nanocomposite grafts as discussed below. These surfaces were also characterized using atomic force microscopy (AFM) on these films on a silicon wafer. These experiments were carried out by Mr. Albert Wan of the Batteas group who found that after these two layers the surface had a thickness of 23 ± 3 nm and a roughness of 6 ± 2 nm.

Preparing Responsive Glass/(PNIPAM/SiO_2)$_6$/PNIPAM Nanocomposite Glass Slides by Covalent Layer-by-Layer Assembly

Nanocomposite grafts on glass surfaces were prepared from a primed glass surface by grafting PNIPAM-*c*-PNASI copolymers and aminated 10 and 100 nm silica particles to an amine modified surface to covalently assemble thin films with responsive wettability. This assembly process took advantage of PNIPAM's temperature responsiveness to create a temperature responsive surface and used silica nanoparticles to increase surface roughness and enhance that response.[80] These syntheses used a copolymer of PNIPAM-*c*-PNASI as the

polyvalent electrophile with the PNASI serving as an electrophile for the amine groups already attached to the prior layers grafted to the glass surface. As was true in the priming step, steric constraints associated with surface reaction preclude consumption of 100 % of the NASI groups in this surface amination chemistry; thus, the remaining active esters produce an electrophilic surface from the previously nucleophilic surface. Subsequent reaction using aminated 10 and 100 nm silica nanoparticles as polyvalent nucleophiles then covalently coupled these nanoparticles to the surface via amide bonds. Again, incomplete reaction of the amino groups lead to a surface with unreacted amine groups that effectively made the electrophilic surface nucleophilic for subsequent grafting steps in this covalent layer-by-layer assembly process. At this point the surface contains both amino groups, some amide groups, and possibly some unreacted NASI groups. Therefore, the surface was then treated with an excess of isopropylamine to convert any unreacted NASI groups to NIPAM groups. This process increases the PNIPAM content of the surface but more importantly removes a reactive site that could over time react and change the surface (Scheme 7).

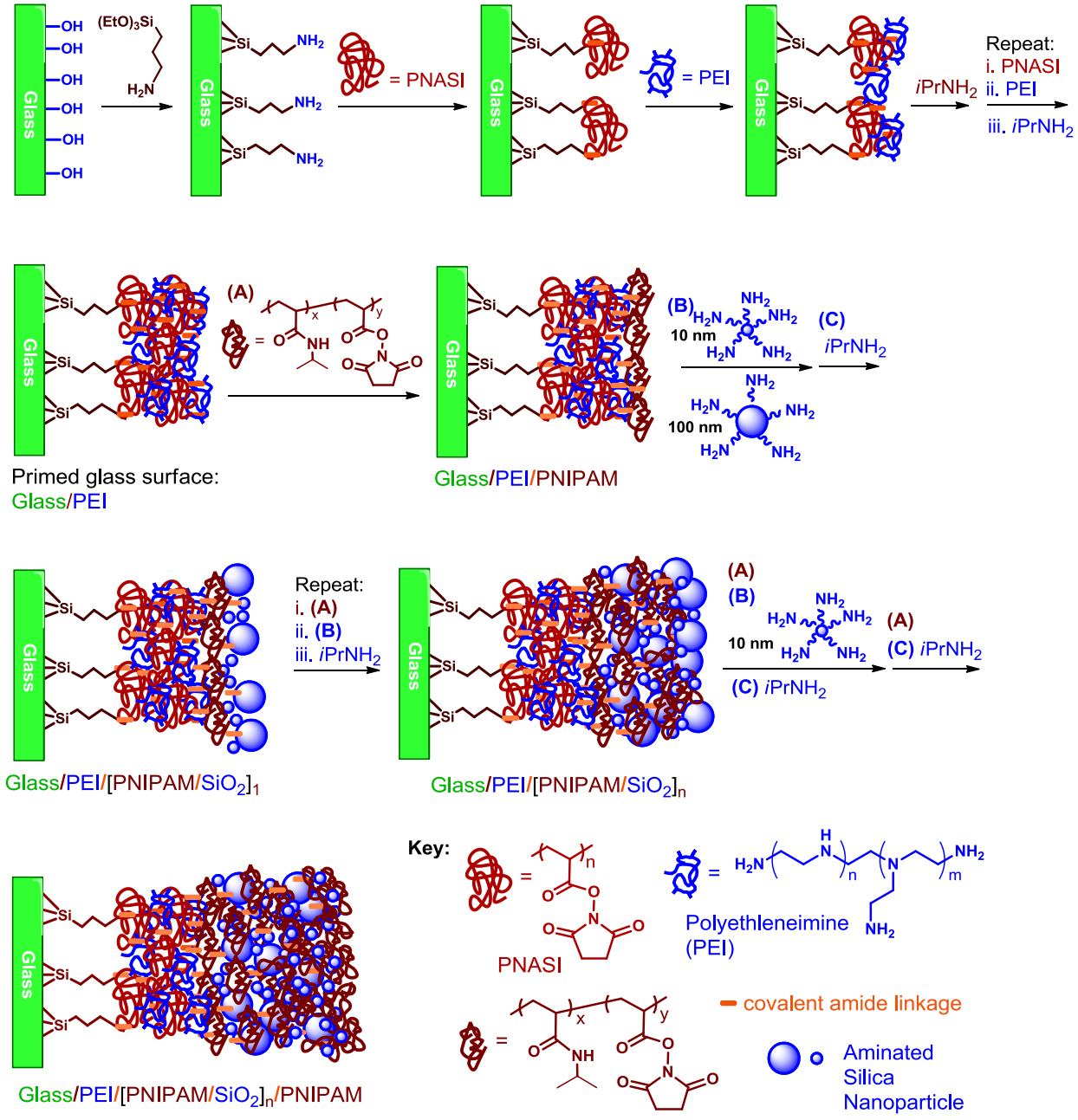

Scheme 7. Synthesis of Glass/PEI/[PNIPAM/SIO_2]$_n$/PNIPAM.

At this point the success of the initial attachment of the polymer and nanoparticles to the glass substrate was evaluated by contact angle measurements using both water and 1.2 M Na_2SO_4. The observed advancing contact angle changed from 75° with water to 120° with 1.2 M Na_2SO_4 which was comparable to the low advancing contact angle of 105° observed using 1.2 M Na_2SO_4 on one layer of the same nanocomposite surface previously built on a silicon wafer. The LbL assembly was continued through four more cycles as shown in Scheme 7. After a five layer nanocomposite formed using PNIPAM-*c*-PNASI/aminated 10 and 100 nm silica/$NH_2CH(CH_3)_2$ treatment steps, a final sixth cycle was carried out using only 10 nm aminated silica to decrease the outermost surface roughness and ensure the top layer would be saturated with PNIPAM. This was followed by a final step with just a PNIPAM-*c*-PNASI copolymer treatment followed by reaction with isopropylamine to ensure the topmost layer was covered with PNIPAM. The finalized graft is referred to as glass/$(PNIPAM/SiO_2)_6$/PNIPAM in this thesis.

Mr. Albert Wan of the Batteas group also measured the roughness and thickness of each of these layers. His results are shown in Table 1. He found that as the number of layers increased, both the surface roughness as well as the contact angle of 1.2 M Na_2SO_4 also increased. The trend was approximately the same until the last 10 nm SiO_2 layer was added which did not have a significant impact on the contact angle.

Table 1. Roughness and thickness of PEI/[PNIPAM/SiO_2]$_n$/PNIPAM on silicon.

	Layer 1	Layer 2	Layer 3	Layer 4	Layer 5	Layer 6 (10 nm SiO_2 only)
Roughness (nm)	93 ± 27	108 ± 36	196 ± 43	216 ± 18	246 ± 86	288 ± 95
Thickness (μm)	0.3 ± 0.1	1.1 ± 0.1	1.2 ± 0.1	1.6 ± 0.1	2.2 ± 0.4	2.4 ± 0.4

The responsive characteristics of the fully constructed surface were assessed by measuring contact angles and are discussed in detail in the next chapter. However, an important consideration in these experiments and in the subsequent experiments to modify frits proved to be a purely mechanical problem. Specifically, surface damage from shaking was a problem encountered in this work that was not encountered in reactions on PE films. For example in the initial studies of this grafting chemistry, reactions for the glass slides were carried out within glass vials on a wrist action shaker. This process led to glass slides with a responsive wettability but also caused high standard deviations between contact angle measurements and apparent inhomogeneities in the surface coverage. These problems and the lack of homogeneity, were attributed to surface damage during shaking due to small pieces of glass that break off on shaking and damage the surface of the glass slides used in these reactions. The tiny glass chips were theorized to create scratches on the chemically robust but physically delicate thin film as indicated by areas of the nanocomposite graft which would absorb the water or salt solution used for contact angle analysis. To avoid this problem, we used a chemically inert Teflon holder to prevent the edges of the glass slide from breaking. This apparatus is shown in Figure 6. With the new holder, surface edges

were protected and the LbL assembly could be carried out to form responsive surface grafts with more consistent contact angles.

Figure 6. Teflon holder used to secure glass slides during functionalization.

Preparing Responsive Glass/(PNIPAM/SiO_2)$_6$/PNIPAM Nanocomposite Grafts on Glass Frits by Covalent Layer-by-Layer Assembly

Glass frits of medium porosity, pore size 10-20 μm, were grafted with SiO_2/PNIPAM nanocomposite grafts using the same covalent layer-by-layer assembly as used to prepare responsively wettable glass slides. However, because the porous glass breaks and chips more easily than glass slides, physical damage during the physical shaking used during the grafting process was even more problematic. First the Teflon holders shown in Figure 7 were

examined. However the exposed surface area for frits in this holder led to frits with only partial functionalization. Eventually, the frit holder in Figure 7(c) was designed. This holder provides the most even surface functionalization based on contact angle analysis on the center compared to the sides of the frits.

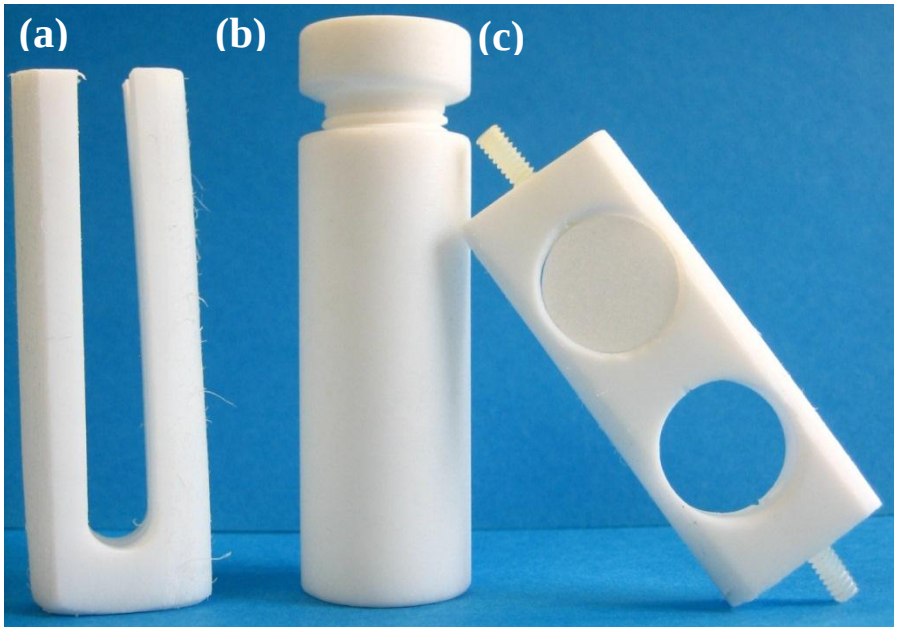

Figure 7. Teflon holders designed to secure glass frits during the functionalization process.

The Figure 7(c) holder was made of Teflon, but in order to achieve maximum exposed frit surface area, nylon screws were utilized on either end to hold the frits in the holder. This holder went through the entire functionalization process, but the nylon screws were removed during the use of piranha solution for cleaning.

Attempted Characterization Methods of Glass Frits

Several attempts to determine the relative amounts of responsive polymer on the individual frits were made. This first used Raman spectroscopy. However, in this case we obtained spectra of both an un-functionalized frit and a fully functionalized glass frit. While subtraction of the former spectrum from the latter spectrum could in principle provide information about the nanocomposite on the frit, in practice scattering of the laser was determined to be too high to collect useful data.

We also pulverized a functionalized frit and attempted to carry out IR analysis on the resulting powder. In this case the intense silicon peak observed in the spectra prevented any detailed analysis of other peaks. While this experiment was unsuccessful, identification of the organic components of the nanocomposite grafts might still be possible in future work if these powders were treated with fluoride to decompose the silica.[96, 97]

When functionalized glass slides were sonicated in solution for 10 min, the once opaque slide appeared "clean" to the naked eye, which indicated at a minimum the removal of the LbL assembled surface. Therefore, glass frits were sonicated in deuterated chloroform so that ^{1}H NMR could be done on the resulting solution. However, no spectral peaks were observed, most likely because the polymers were still bound to the silica nanoparticles.

Conclusion

In conclusion, it was determined that a covalent layer-by-layer assembly process could be used to functionalize a nanocomposite graft on a glass slide as well as on a more three-dimensional surface, a glass frit. These thin films incorporated PNIPAM, a

temperature responsive polymer, as well as silica nanoparticles, to enhance the temperature response and increase surface roughness. It was difficult to characterize the final product on the glass frits because of the natural scattering properties of glass and the roughness of the frits. Therefore the polymers were characterized before attachment to the surface by NMR and the surface's wettability in water and in 1.2 M Na_2SO_4 was used to determine successful binding of PNIPAM to the glass slide. The success of the nanocomposite graft formation on frits was evaluated by passive permeation experiments discussed in Chapter III.

CHAPTER III

MEASUREMENT AND ANALYSIS OF THE RESPONSIVENESS OF POLY(*N*-ISOPROPYLACRYLAMIDE)/SILICA FUNCTIONALIZED GLASS

Introduction

Smart surfaces are surfaces functionalized with responsive polymers which respond to a variety of stimuli such as pH, a change in ionic potential, a change in solvent, or a change in temperature. Poly(*N*-isopropylacrylamide) (PNIPAM) may be grafted by the synthesis of polymer brushes that are initiated from the surface or by preparing the polymer before attaching it to the surface. One way of attaching a preformed polymer is in a layer-by-layer (LbL) assembly by using covalent ionic or hydrogen bonds. PNIPAM's temperature response is due to its conformational change above and below its lower critical solution temperature (LCST) of 32 °C. Below the LCST, the polymer is spread out in a random coil conformation that is easily solvated. Above the LCST the polymer changes to a hydrophobic globular conformation. When PNIPAM is bound to a surface by synthesis of PNIPAM polymer brushes or by an LbL assembly process, it creates surfaces with responsive wettability. These responsive surfaces may be used to mimic the self-cleaning properties of a lotus leaf, bird feather, and insect wing.[98]

Reversible hydrophobic/hydrophilic wettability properties can be assessed by measuring the contact angle of water on a surface. The contact angle is defined in Figure 8 below.

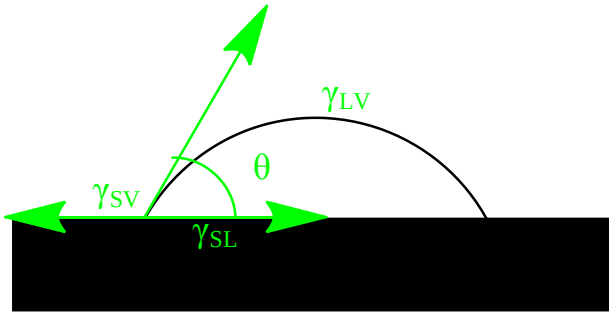

Figure 8. Contact angle measurement and variables defined.

Young's equation uses the variables for surface tension shown in Figure 8, γ_{LV}, γ_{SL}, and γ_{SV}, to rationalize the contact angle from a thermodynamic equilibrium perspective. In this equation L, V, and S stand for the interfaces involving the liquid, vapor and solid phases respectively.

$$\gamma_{LV}\cos\theta = \gamma_{SV} - \gamma_{SL}$$

The contact angle of water is used to define the surface's wettability. The surface is hydrophilic when the contact angle (θ) is less than 90°; above 90° the surface is hydrophobic. Typically surfaces which have contact angles above 150° are considered superhydrophobic while surfaces possessing contact angles less than 30° are considered superhydrophilic.[80]

For rough surfaces however, it is difficult to know exactly how the contact angle is affected. There are two models to describe how the contact angle is affected by surface roughness. The Wenzel model proposes that the drop is in full contact with the surface.[99] Because the surface liquid contact is unfavorable for a hydrophobic surface, the angle is

amplified to reduce surface liquid interaction. The amplification due to surface roughness is shown in the following equation and Figure 9.

$$\cos\theta' = r\ \cos\theta$$

The contact angle θ' is the apparent contact angle of a surface that has a flat contact angle of θ but also has a surface roughness of r.

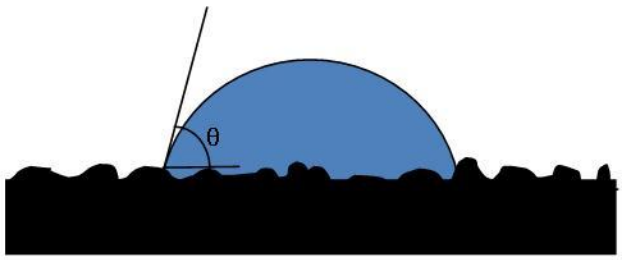

Figure 9. Contact angle on a rough surface using Wenzel's model.

Another model, developed by Cassie and Baxter attributed this amplified contact angle (in the following equation – θ_{12}), to a combination of the effect of the flat surface contact angle with the effect of the contact angle in air.[93]

$$\cos\theta_{12} = f_1\cos\theta_1 + f_2\cos\theta_2$$

In this case, f_1 is the fraction of contact between the water and the surface, and θ_1 is that surface's contact angle. On a rough surface, f_2 is typically the fraction of contact with air in which case θ_2 is assumed to be 180°. This is shown in Figure 10 below:

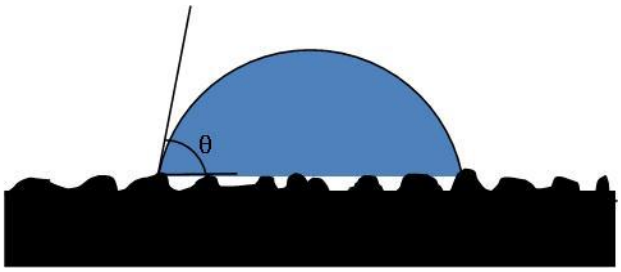

Figure 10. Contact angle on a rough surface using Cassie's model.

Because the surface tension between a new nanocomposite graft and the liquid drop is unknown, a goniometer is used to measure the contact angle and does so by taking a picture and using variances in pixel color to find the edge of the drop and graphically determine a contact angle.

When these responsive polymers are grafted to nanoporous membranes, they may be used for microfluidic sensors, controlled delivery systems, or smart filtration devices.[12, 100] Smart polymers grafted to nanopore walls may be used to control the opening and closing of the nanopores by controlling the surface wettability.[12] The flow rate through the pores is a combination of a physical response to the size of the polymer and a chemical response to the repulsion of water molecules by a hydrophobic surface.[101] When the responsive polymer graft utilized PNIPAM, the functionalized pores become impermeable to water when PNIPAM is in its globular, hydrophobic conformation, above its LCST.

Schepelina and coworkers grafted a nanoporous colloidal film with PNIPAM using atom transfer radical polymerization (ATRP). The thickness of polymer synthesis on the surface has a crucial effect on the permeability of the membrane.[101] When the polymer was able to fill the entire void, they postulated that the initiators allowed it to crosslink across the

pore.[101] When the polymer was given enough reaction time it became long enough to crosslink into a mesh across a nanopore. Water was still able to penetrate through the mesh below the LCST of PNIPAM.[101] When the temperature was above the LCST, the water was unable to penetrate because the mesh across the pore became hydrophobic.[101]

This study was done by measuring the flow rate of water through a PNIPAM grafted surface in response to temperature. Surface wettability studies using contact angle measurements on solid substrates have been conducted to determine how PNIPAM responds to sodium sulfate and other anions in the Hofmeister series.[51] The Hofmeister series scales the ability of salt anions to desolvate a protein molecule. Anions originally known as kosmotropes, for the belief that they would break the water structure surrounding solvated proteins, have a "salting-out" effect on PNIPAM. When PNIPAM was grafted to polyethylene films, Liao and coworkers measured the contact angle with solutions of the Hofmeister series salts. Drops of kosmotropic salts such as sodium sulfate or sodium citrate were measured to have contact angles near 140° at concentrations of 1.0 M. Water droplets on the functionalized surface exhibited contact angles near 76°. The grafts were reversibly hydrophilic and hydrophobic to kosmotropic salt solutions and water respectively. Chaotropic salts on the other hand, yield a "salting-in" effect and have a much smaller influence on the LCST. Therefore drops of chaotropic salts had contact angles near 72°, close to that of water.

It was anticipated the effects of these anions as seen in solution and on PNIPAM functionalized polyethylene surfaces could be extended to change flow rates through

functionalized glass frits. This proved to be true and flow rate changes up to 3 orders of magnitude were observed using both temperature and solute identity as the external stimuli.

Surface Responsiveness on Glass Slides

Glass slides were functionalized in accordance with a layer-by-layer assembly of PNIPAM/SiO_2 nanocomposite graft as discussed in Chapter II to create a surface with responsive wettability. These responsive surfaces on the glass slide were synthesized within a u-shaped Teflon holder. To verify the formation of a responsive surface, contact angle measurements were taken with a goniometer of several points on the glass using droplets of water and a solution of 1.2 M Na_2SO_4 and then averaged. The respective contact angles increase from ~77° to 170° when water to sodium sulfate were used (Table 2). This change of nearly 100° meant the surface went from hydrophilic to superhydrophobic.

Table 2. Average contact angles for droplets of water and 1.2 M Na_2SO_4.

Sample	Water	1.2 M Na_2SO_4
Slide A	73.58	> 170
Slide B	84.13	> 170

Because the nanocomposite graft in the presence of sodium sulfate was very hydrophobic, contact angles could not be measured. A drop increasing in size at 0.1 µL/s during the advancing contact angle measurement is shown in Figure 11. A 180° contact angle would be a completely hydrophobic surface. The weight of the solution caused the

drop to deform while maintaining a high contact angle before increasing the solution's contact area with the surface, and the droplet deformation made the contact angle immeasurable. Due to approximate contact angle values, standard deviations for 1.2 M Na_2SO_4 were not able to be calculated. The contact angles of water on Slide A & B had standard deviations of 4.77 and 5.56 respectively.

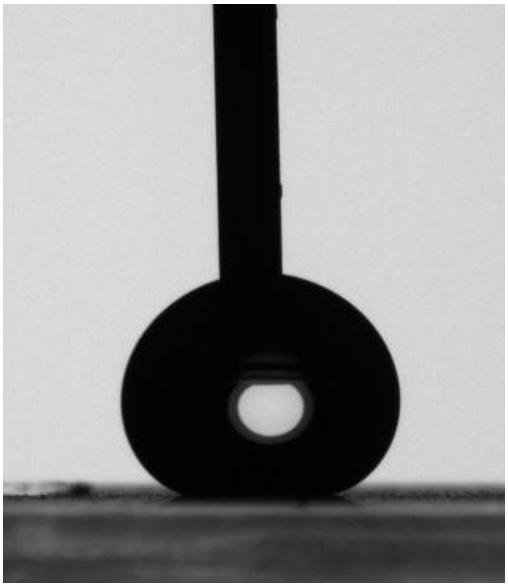

Figure 11. Image taken during advancing contact angle measurement of 1.2 M Na_2SO_4 on a functionalized glass slide.

The observed changes in contact angle were reversible, showing that the surface was able to exhibit both hydrophilic and hydrophobic properties. Sodium sulfate is able to lower the LCST of the surface bound PNIPAM so that the polymer undergoes a change from the coil to globular conformation. When PNIPAM is in the globular conformation, it is hydrophobic. The LCST reverts back to 32 °C when the salt solution is removed and the slide is washed with 18 MΩ water and thoroughly dried. When a water drop is placed on the surface it will again exhibit hydrophilic properties at room temperature.

Using Contact Angles to Determine Surface Responsiveness of PNIPAM/SiO_2 Functionalized Glass Frits

In order to investigate the surface responsiveness of functionalized glass frits, contact angles were measured. Glass frits were also functionalized with a PNIPAM/SiO_2 nanocomposite graft as discussed in Chapter II. A functionalized glass frit, frit 1, was first tested by measuring the contact angle of sodium sulfate solutions ranging from 0.0 to 1.2 M over a maximum of twenty minutes. The frit was washed and dried between each measurement. The extended time in these measurements allowed the change in contact angle

to be observed as the drops penetrated into the frit. Increasing concentrations of sodium sulfate were measured to assess the ability of the nanocomposite graft to control the flow rate and the dependence of that ability on sodium sulfate concentrations. The functionalized frit clearly showed a concentration dependence which is depicted Figure 12. Lower concentrations of sodium sulfate were able to completely penetrate the frit at a much faster rate than the higher concentrations above 0.6 M Na_2SO_4 which did not penetrate the frit. This solute responsiveness of the nanocomposite graft is due to the decrease in the LCST by the sodium sulfate. Sodium sulfate lowers the LCST below room temperature, and the surface was therefore hydrophobic at room temperature; so at high concentrations the solution is unable to enter the glass frit. As the concentration of sodium sulfate increased, the hydrophobicity of the frit also increased. This was valuable information because it showed an approximate concentration at which the sodium sulfate droplet would no longer penetrate into the pores of the frit. Both the sodium sulfate and 18 MΩ water droplets completely penetrate into un-functionalized frit in approximately 1 s.

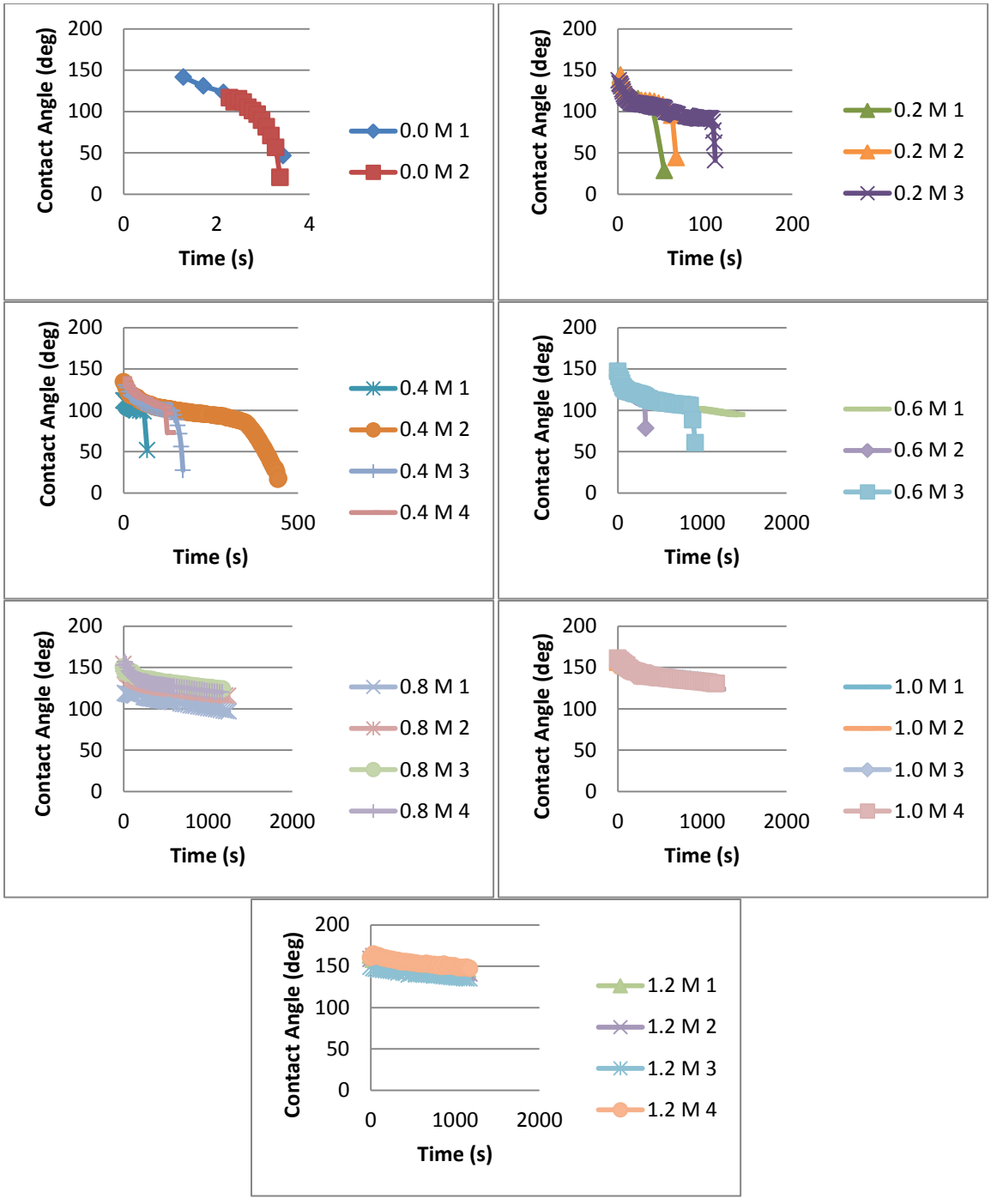

Figure 12. Contact angle measurements on functionalized glass frit 1 with increasing concentrations of Na_2SO_4 from 0.0 to 1.2 M.

At concentrations above 0.6 M Na_2SO_4, static contact angles of 10 µL droplets typically decreased less than 30°. Similar changes in contact angle were observed on a glass slide over this extended period of time and a comparison can be seen in Figure 13.

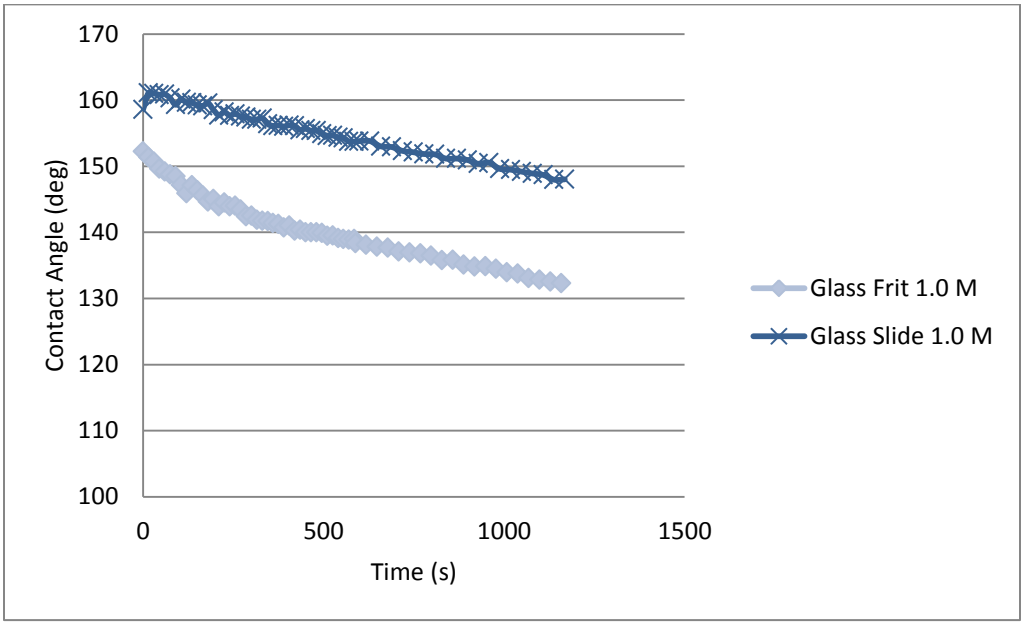

Figure 13. Comparison of 1.0 M Na_2SO_4 on a glass slide for 20 min to 1.0 M Na_2SO_4 on a frit for 20 min.

The slight decrease in contact angle, such as those seen at 0.8 M, 1.0 M, and 1.2 M Na_2SO_4 concentrations in Figure 12, was attributed to the time it took the surface to rearrange.[82] Although a sharp coil to globule transition is observed, over approximately 0.5 °C in solution, Liu and coworkers found that for PNIPAM brushes bound to a surface the phase transition would occur from 20 to 38 °C.[14, 83] There is a significant decrease in the ability of the polymer to remain hydrophobic between concentrations of 0.6 M and 0.4 M Na_2SO_4. This range of concentrations was determined to be the break-through concentration

range for sodium sulfate solutions on a functionalized frit. Between the sodium sulfate concentrations of 0.6 M and 0.4 M, the droplets had high deviations in the amount of time it took to penetrate the frit. The droplets for concentrations below 0.8 M Na_2SO_4 were observed to have a steady decrease in contact angle until a few seconds before total penetration. At that point the rate at which the drop entered the frit increased, therefore changing the contact angle at a faster rate. The sharp transition at which the drop of low concentration sodium sulfate solutions enter the frit was considered to be an effect of capillary forces of the three dimensional structure. Once the drop begins to enter the frit, capillary action could theoretically take over and aid in pulling the remaining solution into the frit despite the functionalized hydrophobic surface. The increasing hydrophobicity of the surface due to increasing concentrations of sodium sulfate indicated that the frit had been successfully functionalized.

Using Flow Rates to Determine Surface Responsiveness of Glass Frits

After it was determined that the frits had been successfully functionalized flow rate measurements were conducted to better assess the ability of the nanocomposite graft in preventing the penetration of sodium sulfate solution, as well as the extent of reversibility of the wetting response. To do this, frits were placed in a Teflon chromatographic column to tubing adapter. By attaching the Teflon adapter to a column and filling it with water or salt solutions, flow rates of 1 cm of water or solution were measured. The centimeter measured was always from ~5 cm to ~4 cm above the top of the frit. This was to avoid any variation in flow rates due to changing hydrostatic pressures which are dependent on the liquid height

above the frit. At the start of the experiments to determine the reversibility of flow rates for water and sodium sulfate solutions the washing cycle in between experiments was not strictly regulated. The results showed reversibility with poor control of the water flow rates, indicated by a relative standard deviation 37 %. Thus, strict control over the washing and drying process between the experiments was necessary. The variation in flow rates obtained when washing steps were not regulated was very likely due to the strong hysteresis of the polymer when it is bound to a surface, as proved by Liu and coworkers.[83]

With careful modification of the experiment to standardize the water washing, water flow rates, methanol rinsing, and nitrogen drying time, the frits were determined to exhibit reversible permeation between high concentrations of sodium sulfate and water. At concentrations of sodium sulfate greater than or equal to 0.8 M, the solution would not permeate a functionalized frit during a minimum testing period of 12 h. After a frit was in contact with a sodium sulfate solution, it was first rinsed 4 times with 50 mL of water. Then the surface rinsed frit was washed by allowing approximately 3 cm of water to pass through the frit. The next 1 cm that passed through the frit was used to measure a water flow rate. Several examples of this reversibility are shown in Figure 14.

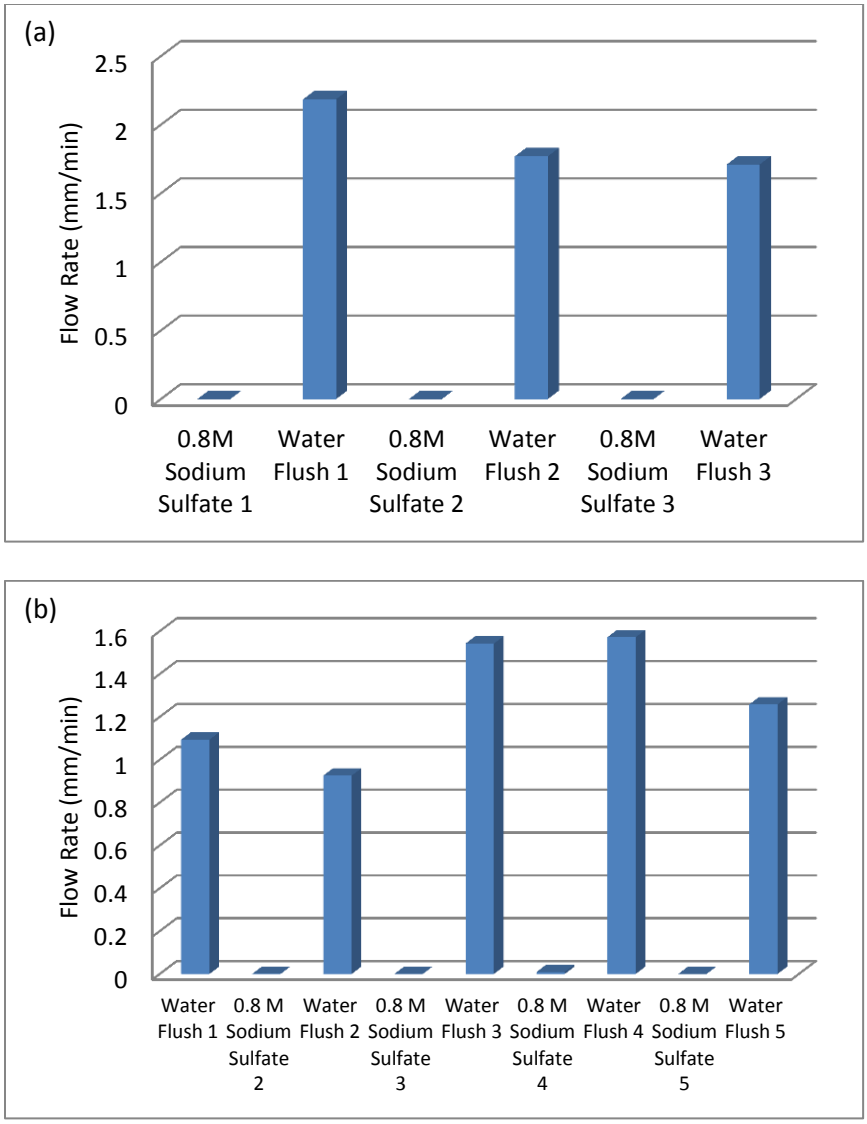

Figure 14. Reversibility of 0.8 M / 1.2 M Na_2SO_4 and 18 MΩ water. (a) Frit 2 showing 0.8 M. (b) Frit 3 showing 0.8 M. (c) Frit 4 showing 0.8 M. (d) Frit 5 showing 0.8 M. (e) Frit 6 showing 0.8 M. (f) Frit 7 showing 1.2 M.

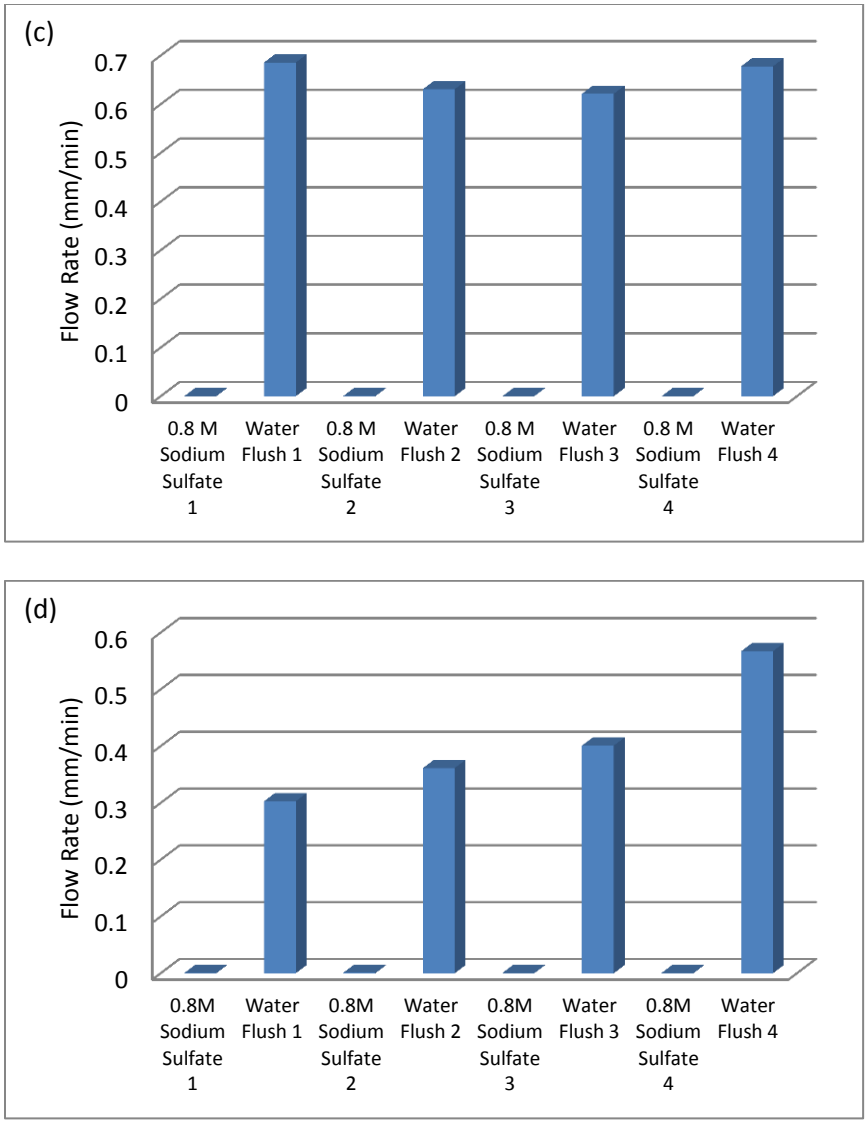

Figure 14. Continued.

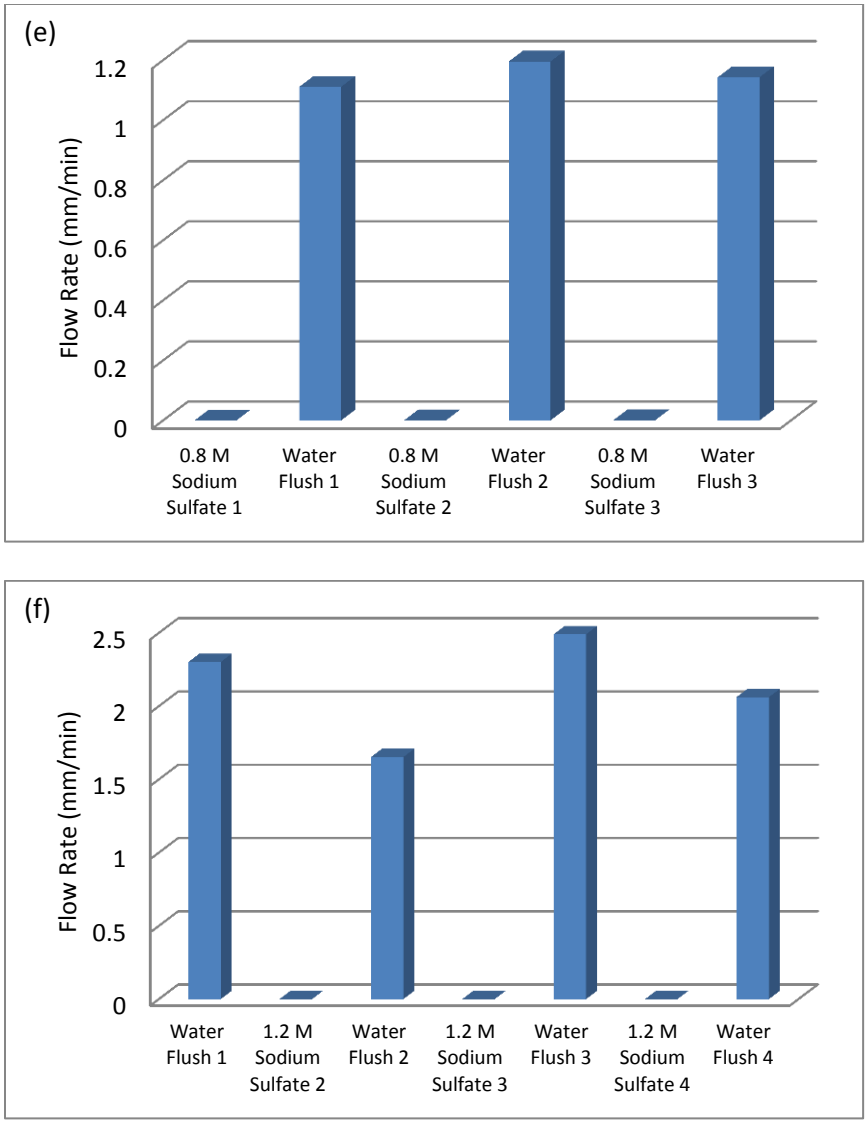

Figure 14. Continued.

High concentrations of sodium sulfate were unable to permeate the functionalized frit due to the globular and hydrophobic properties of the nanocomposite graft under these salt conditions. To test the effectiveness of preventing permeation of 1.2 M Na_2SO_4 through a functionalized frit, the sodium sulfate solution was left on the frit for over 72 h and was

found to not penetrate. The reversibility of flow rates between water and high concentrations of sodium sulfate was tested 3 or more times for each frit. It was found that the water flow rates of different frits varied substantially, but flow rates on the same frit remained constant with relative standard deviations typically less than 25 %.

Because of the known changes in the wettability of PNIPAM grafted surfaces due to anions in the Hofmeister series, 0.8 M sodium citrate, another kosmotropic salt, was also tested in the same manner as sodium sulfate and found to induce the same controllable permeation effect. The reversibility for two frits under this condition can be seen in Figure 15 below.

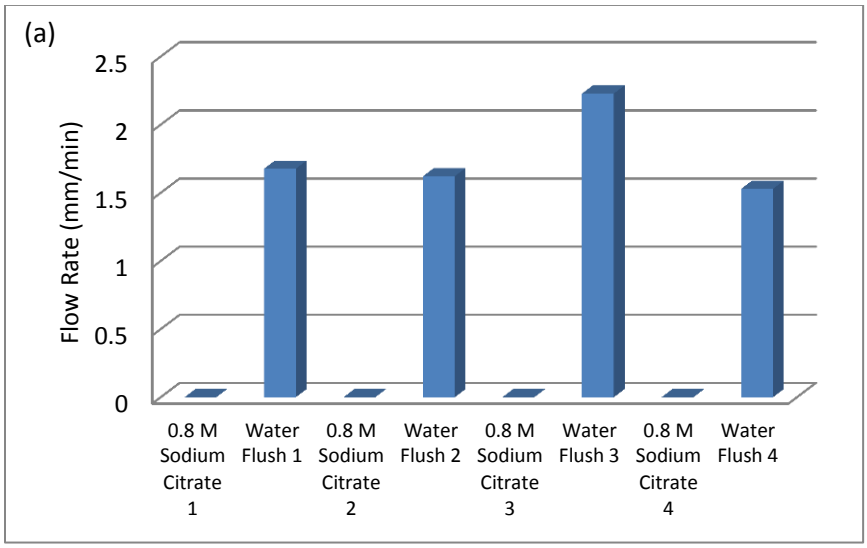

Figure 15. Frits 2 (a) and 3 (b) showing the reversible flow rates of 0.8 M Na_3Citrate and 18 MΩ H_2O.

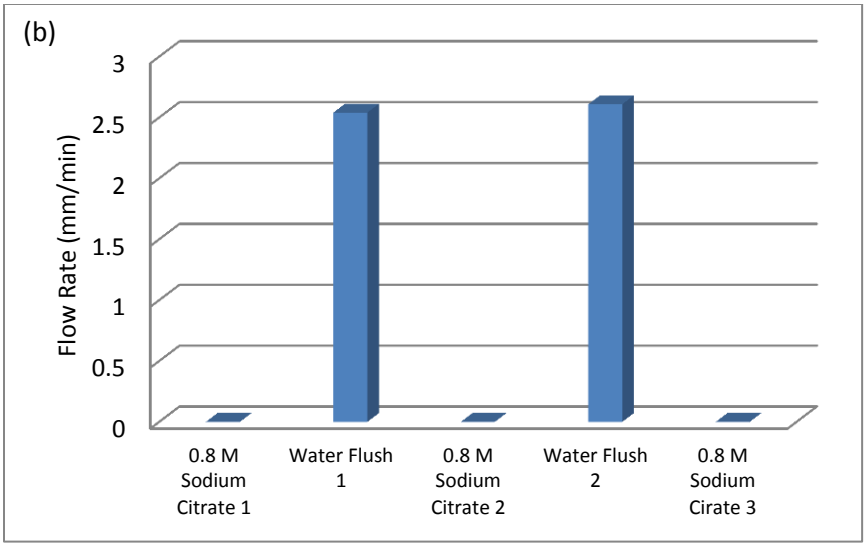

Figure 15. Continued.

At the opposite end of the Hofmeister series, sodium thiocyanate, a chaotropic salt, was hypothesized to flow at rates similar to water. For frit 5, water had an average flow rate of 0.41 mm/min compared to 0.35 mm/min for sodium thiocyanate. The flow rates of NaSCN are represented graphically in Figure 16.

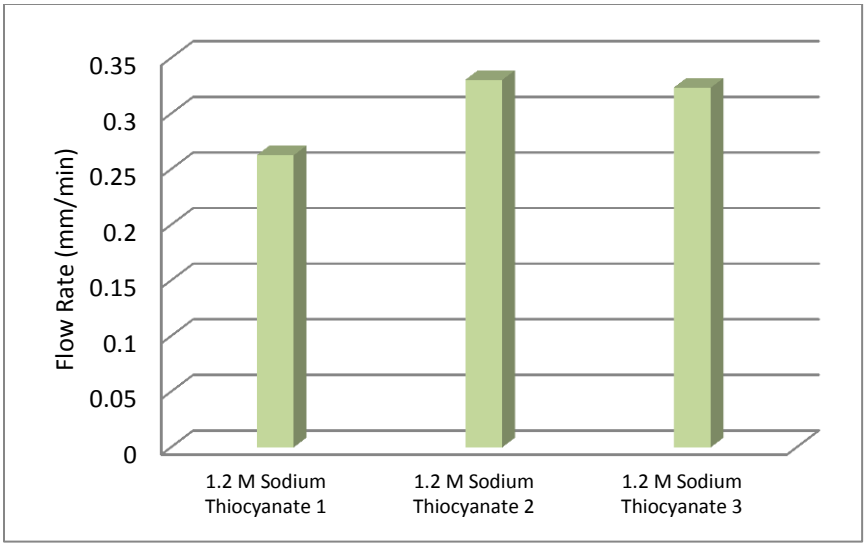

Figure 16. Flow rates of 1.2 M NaSCN on frit 5.

Breakthrough Concentrations of Sodium Sulfate Solutions on Functionalized Frits

Once it was established that frits functionalized with PNIPAM/SiO_2 nanocomposite grafts exhibited the same responsiveness to the Hofmeister series as a solid surface, it was determined that concentrations near 0.6 M Na_2SO_4 would allow the solution to flow the 1 cm through the frit in less than the 12 h time constraint. However, for frits 5 and 7 the breakthrough point was closer to 0.4 M Na_2SO_4 (Figure 17). The variation in the concentration which sodium sulfate was able to penetrate the frit was still within the range observed for drop penetration when measuring the contact angles.

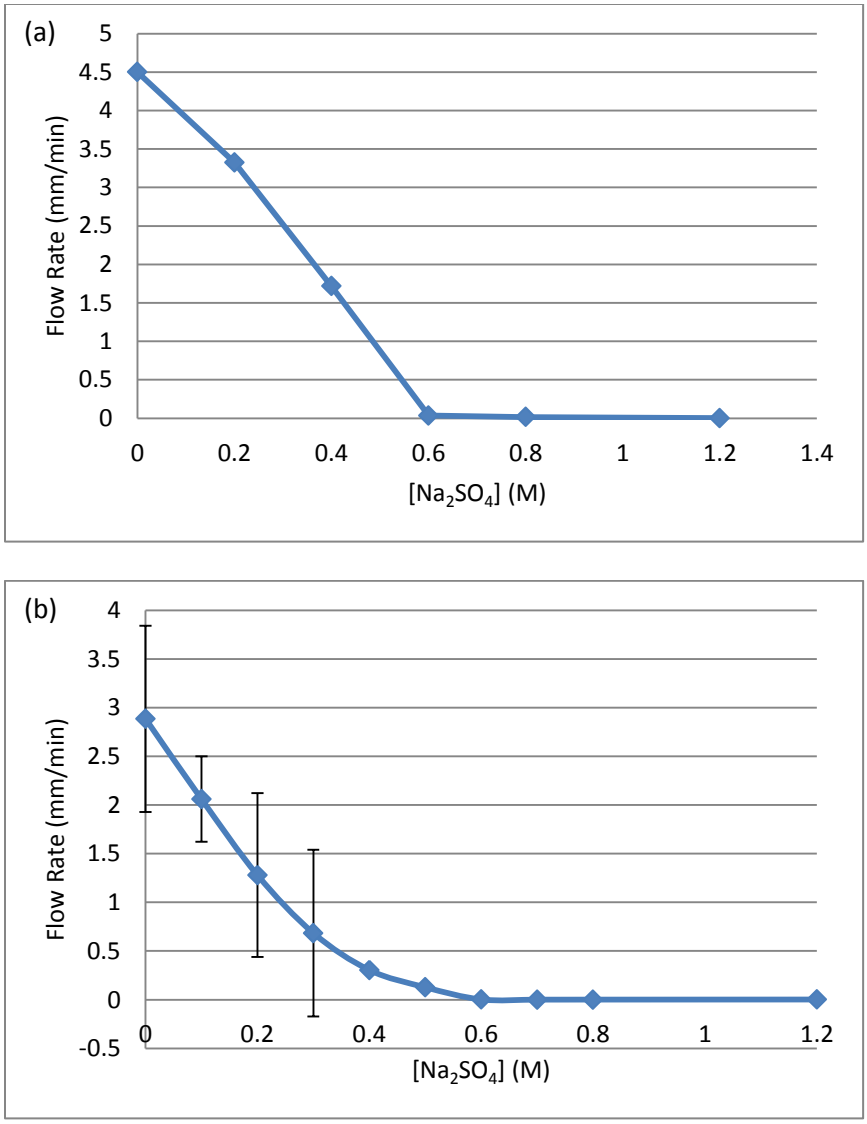

Figure 17. Comparing flow rates of several Na_2SO_4 concentrations on a single frit. (a) Frit 1. (b) Frit 3. (c) Frit 5. (d) Frit 8. (e) Frit 9.

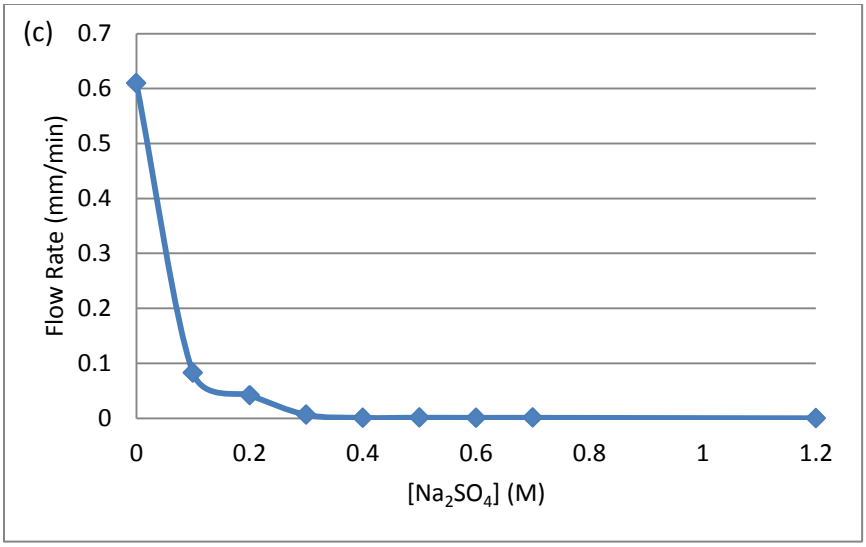

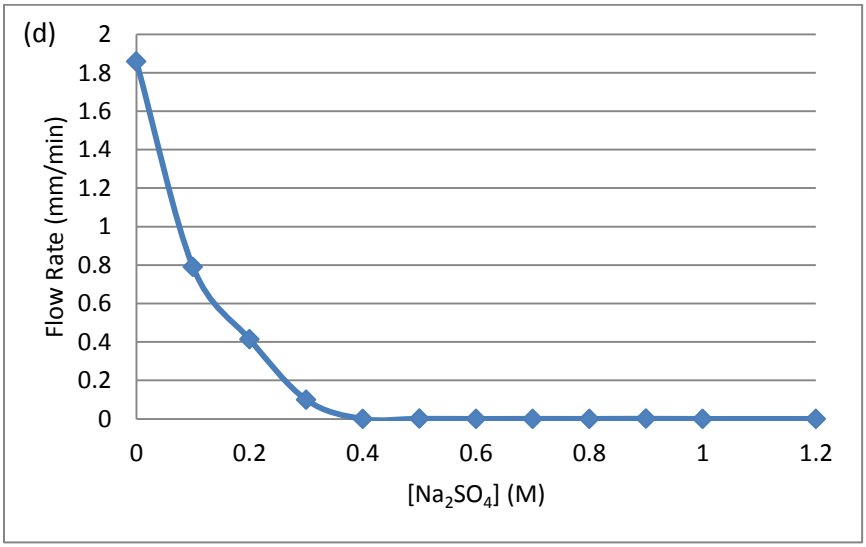

Figure 17. Continued.

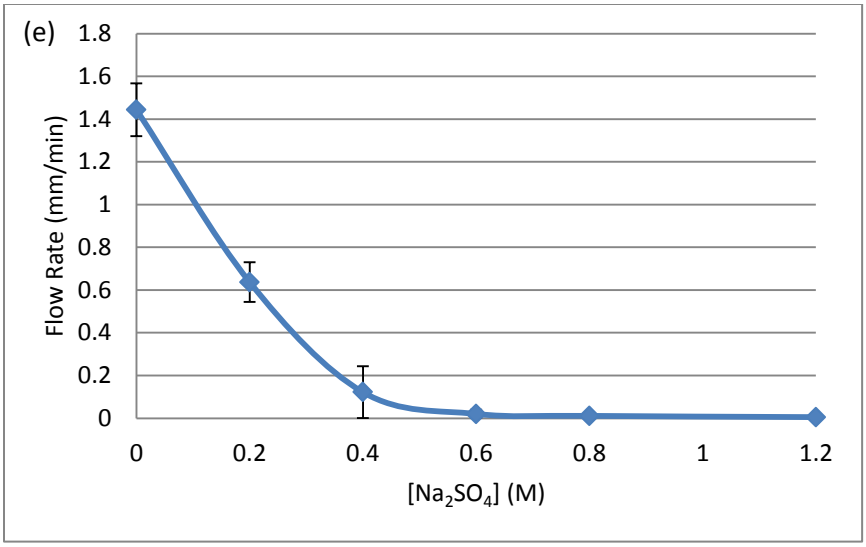

Figure 17. Continued.

Due to the hysteresis of PNIPAM especially when it is bound to a surface, gathering data with changing concentrations and the same washing and drying procedure did not allow the PNIPAM enough time to equilibrate as well as it did during the reversibility experiments. A high amount of error was observed when flow rate experiments were repeated for low concentrations of sodium sulfate on the same frit. This is shown in Figure 17(b). The curves typically showed breakthrough points between 0.4 M and 0.6 M Na_2SO_4 which was consistent with the results observed when measuring the contact angles on a functionalized frit. In order to achieve more reproducible flow rates for the lower concentrations, the washing process of the frits was altered to allow the polymer to revert back to its coil conformation to a greater extent, therefore reducing the observable error, as seen in Figure 17(e). The frits were submerged in cold water which was stirred with an overhead stirrer in a cold room around 7 °C for 3 h after each test. The drying time therefore was increased to 4

h. Whenever the PNIPAM/SiO_2 nanocomposite graft comes in contact with sodium sulfate, the LCST of the PNIPAM was decreased. Cooling the surface in solution below the LCST of PNIPAM in the presence of sodium sulfate allows the polymer to revert back to its chain conformation due to a temperature stimulus as the graft on the frit is cooled as well as a solute stimulus as the salt solution is washed away.

One attempted measurement of a breakthrough curve led to information which supported the theory that capillary action draws the solution into the frit. The involvement of capillary action was first observed through the slope change when measuring contact angles of penetrating drops on a functionalized frit. The experiment was done by measuring the flow rates of increasing sodium sulfate solutions, from 0.0 to 1.2 M, without washing in between changing solutions. The results are shown in Figure 18. Theoretically, in the presence of sodium sulfate, the PNIPAM grafted to the surface should rearrange to its hydrophobic conformation. Despite this assumed rearrangement when the frit was already wet, sodium sulfate solutions of both low and high concentrations would continue to flow at similar rates. The consistent flow rates of water through 1.2 M Na_2SO_4 were most likely due to the inability of the repulsion force from the increased hydrophobicity of the nanocomposite graft to overcome the capillary action forces. Further research is needed to determine the extent of these effects.

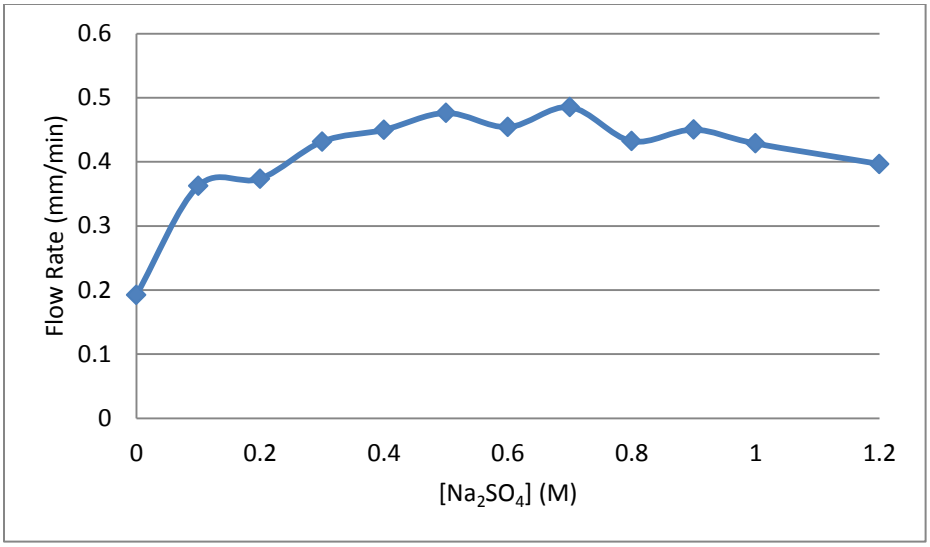

Figure 18. Flow rates on frit 10 of increasing concentrations of Na_2SO_4 measured without washing and drying the frit between different concentrations.

Controlling Flow Rates of Functionalized Frits with Temperature

Just as the flow rate control was due to kosmotropic salts lowering the LCST of surface grafted PNIPAM below room temperature, the reversible flow rates were also observed as a thermal response. Before testing the flow rate at low temperatures, both the solution and the flow rate setup were left in the cold room overnight before each experiment. Because sodium sulfate is only soluble up to 0.48 M at 5 °C, 0.5 M Na_2SO_4 was used to measure flow rates near 7 °C and 23 °C.[102]

Figure 19 shows the flow rates of a 0.5 M Na_2SO_4 solution through a PNIPAM functionalized glass frit above and below its LCST. The flow rates of 0.5 M Na_2SO_4 inside and outside the cold room changed by a factor of 100, despite the slower than water flow rate.

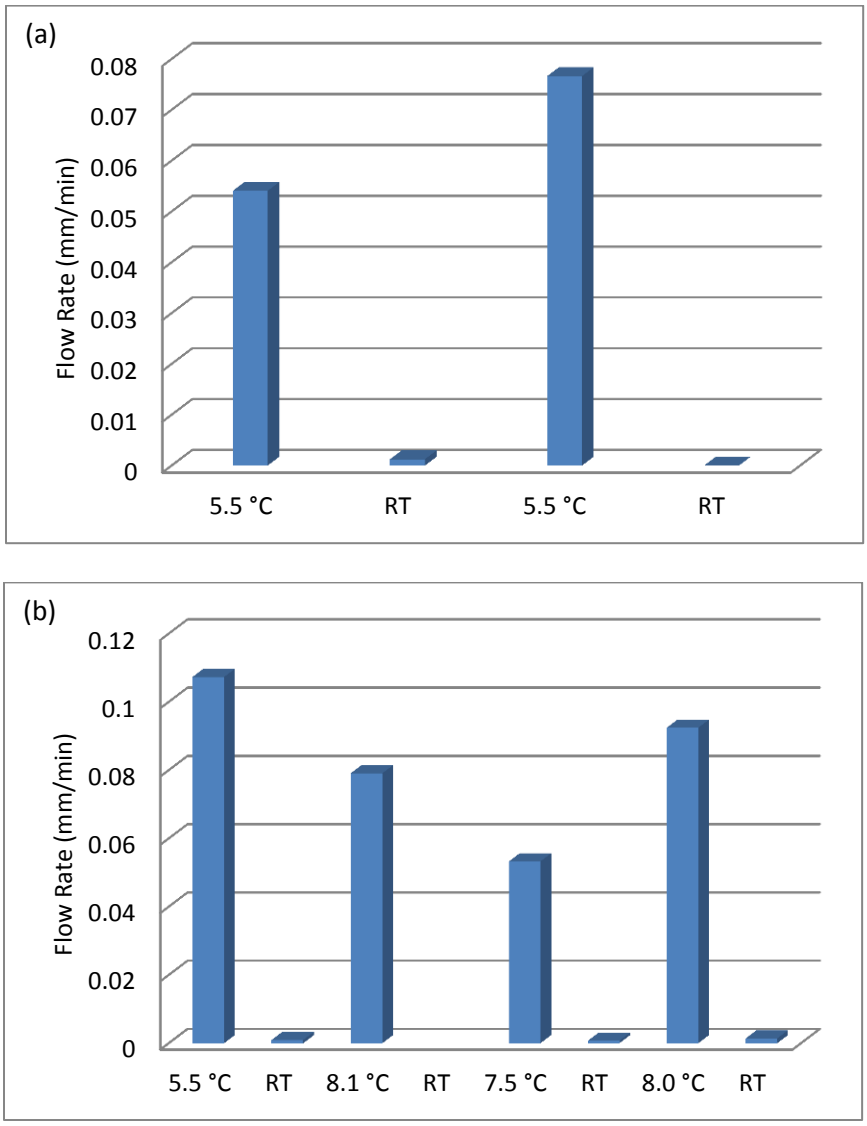

Figure 19. Flow rates of frits 5 (a) and 10 (b) at room temperature (RT) and below the LCST of PNIPAM in the presence of 0.5 M Na_2SO_4.

When the flow rate of 18 MΩ water was measured through these functionalized frits in the cold room and compared to room temperature, the average flow rate remained the same. On frit 10, as shown in Figure 19, the second experimental run at room temperature

was thrown out with 99 % confidence. Such a different value was most likely due to the frit not being fully dry.

It was also attempted to control the flow rate of pure water by increasing the temperature of the solution and the flow rate apparatus above 32 °C. The setup shown previously was connected to a collection tube that could be placed in a water temperature bath and still open to air on the other side. The temperature bath was set at 45 or 50 °C. In the flow rate experiments, the frit was encased in a Teflon holder and therefore heat could not efficiently conduct to the glass frit from the hot water bath. If the glass frit is left at room temperature because it is exposed to air it was hypothesized that it would cool the heated water on contact enough to allow a small amount of water to penetrate the surface of the frit. If this happened, capillary action forces would take over and pull the water all entirely through the frit. The difference in temperature between the glass surface and the water was considered to be the reason for flow rate changes of only factors of 4 to 7. Further research is needed to develop a method to heat the entire apparatus.

Conclusion

By testing salt solutions at both ends of the Hofmeister series, it was determined that frits functionalized with a PNIPAM/SiO_2 nanocomposite graft may be made hydrophobic with kosmotropic salts and remain hydrophilic with water or chaotropic salt solutions at room temperature. Flow rates varied from frit to frit most likely due to measureable differences in the extent of functionalization as well as variability in pore size, 10 – 20 μm. Because the Hofmeister effect seen using sodium sulfate is due to a lowering of the LCST of

PNIPAM, temperate responsiveness of the nanocomposite graft was able to be measured. This was done by comparing 0.5 M Na_2SO_4 flow rates in and outside of a cold room at ~7 °C. Flow rates were found to change by approximately 2 orders of magnitude. The breakthrough concentration of sodium sulfate proved to be between 0.4 and 0.6 M and supported the theory that capillary action forces did effect the flow rate was observed in contact angle measurements on the frit. It was also determined that precise washing and drying was needed between each of these measurements due to the hysteresis of the surface bound PNIPAM.

CHAPTER IV

SUMMARY AND EXPERIMENTAL

Summary

Temperature responsive PNIPAM, with an LCST of 32 °C, was used to synthesize a nanocomposite graft on glass surfaces. An aminated and primed glass surface was reacted in a stepwise covalent reaction with a copolymer of PNIPAM-*c*-PNASI, followed by reaction with aminated silica nanoparticles in a covalent layer-by-layer assembly process. The PNASI groups of the copolymer served as an electrophilic functional group for part of the covalent amide assembly process and the functionalized silica nanoparticles both roughened the surface and provided nucleophilic amine groups in the second step of this covalent LbL assembly process. When the resulting nanocomposites were synthesized on glass slides, solutions of milli-Q water or water containing 1.2 M Na_2SO_4, a kosmotropic salt, were used to measure the contact angle and the difference in wettability between these two solutions on the surface. This experiment showed the reversible solute responsive wettability of the nanocomposite graft on glass with contact angles that reversibly changed from approximately 79° when using 18 MΩ H_2O to over 170° when using 1.2 M Na_2SO_4.

Medium porosity glass frits with pores ranging from 10 – 20 μm were also functionalized with a PNIPAM/SiO_2 nanocomposite grafts. The frits could not be analyzed by spectroscopy due to their intense scattering. The success of the functionalization of the frit was evaluated by measuring a change in flow rates from using high concentrations (0.8 M and 1.2 M) of sodium sulfate versus flow rates using pure 18 MΩ H_2O. Flow rates for high

concentrations of sodium sulfate as well as sodium citrate changed by approximately 3 orders of magnitude, while flow rates of solutions containing sodium thiocyanate did not change significantly compared to water. These different responses to flow rates for kosmotropic and chaotropic salts from the Hofmeister series showed that the nanocomposite graft responds to solute identity.

Varying concentrations of sodium sulfate showed that the flow rates also depended on the concentration of the salt solution as well. Higher concentrations would not penetrate the frit and concentrations between 0.6 M and 0.4 M Na_2SO_4 and below would penetrate at increasing rates with rates eventually approaching that of pure water. The functionalized frits also responded to a change in temperature. Flow rate changes of approximately 2 orders of magnitude were observed on cooling to 7 °C indicating that the frit permeability not only responds to solute identity but also responds to changes in temperature.

Experimental

Materials and Methods. *N*-hydroxysuccinimide, acryloyl chloride, and polyethyleneimine (M_w = 25,000) were obtained from Sigma Aldrich and used as received. 3-aminopropyltriethoxysilane was obtained from Alfa Aser. *N*-isopropylacrylamide was obtained from Sigma Aldrich and was recrystallized from benzene. 10 and 100 nm SiO_2 were obtained from Sigma Aldrich and Fiber Optic Center Inc. respectively. Silica nanoparticles (2.5 g) of 10 or 100 nm were cleaned in 5 % hydrochloric acid solution (50 mL) by shaking overnight. The suspension was centrifuged and the supernatant solution was removed to recover the particles. The particles were then re-suspended twice in water (50

mL) and once in methanol (50 mL) and collected by removing the supernatant solution. After washing with methanol the particles were dried under vacuum overnight.

A Milli-Q Plus water purification system from Millipore was used to obtain 18 MΩ water. NMRs were taken using an Oxford 300 MHz NMR spectrometer. IR was done using a Nicolet 6700 FT-IR. Raman spectroscopy was done using a WiTec Alpha300 confocal fluorescence/AFM system.

Synthesis of *N*-acryloxysuccinimide (NASI). *N*-hydroxysuccinimide (10.0 g, 87 mmol) was added to a solution of triethylamine (12 mL, 90 mmol) and dichloromethane (130 mL) at 0 °C. Acryloyl chloride (7.50 mL, 92 mmol) was added dropwise, and the resulting suspension was stirred for 20 min before it was removed from the ice bath and allowed to stir for an additional 60 min. The resulting salt was removed by filtration and the filtrate was washed with water (~5 mL) and dichloromethane (~10 mL). The filtrate was washed two times with cold water (80 mL x2) and cold brine (80 mL x2). The combined organic layers were concentrated under reduced pressure. When approximately 10 mL of solution remained, the remaining solution was cooled to 0 °C. A hexanes / ethyl acetate solution (6:1, 25 mL) was added and the suspension stirred for 20 min. The precipitate was collected by filtration and dried under vacuum to yield NASI as a white powder (11.6 g, 80 %). ^{1}H NMR ($CDCl_3$, 300 MHz) δ 1.60 (s, 2H), 2.87 (s, 4H), 6.18 (d, J=17 Hz, 1H), 6.33 (m, 1H), 6.71 (d, J=17 Hz, 1H).

Synthesis of poly(*N*-acryloxysuccinimide) (PNASI). NASI (10.0 g, 59 mmol) and 2,2'-azobisisobutylnitrile (AIBN) (25 mg, 0.15 mmol) were dissolved in benzene (300 mL) under N_2. The solution was degassed then placed in an oil bath at 80 °C and allowed to stir

for 12 h. The product was collected by filtration and dried under a vacuum to yield a white powder (9.5 g, 95 %). ^{1}H NMR (DMSO-d_6, 300 MHz) δ 2.05 (bs, 2H), 2.80 (bs, 4H), 3.13 (bs, 1H).

Synthesis of poly(*N*-isopropylacrylamide-*c*-*N*-acryloxysuccinimide) (PNIPAM-*c*-PNASI). *N*-isopropylacrylamide (NIPAM) (3.6 g, 32 mmol), NASI (0.6 g, 3.5 mmol), and AIBN (0.0262 g, 1.6 mmol) were dissolved in benzene (200 mL). The solution was degassed 3 times by flushing it with nitrogen for 10 min and pulling a vacuum for approximately 10 s, then allowed to reflux for 12 h under N_2 while stirring. After concentration under reduced pressure, the resulting solid was dissolved in 50 mL of tetrahydrofuran (THF) and purified by dropwise addition to ethyl ether (450 mL). The precipitated polymer was collected by filtration and dried under vacuum to yield the PNIPAM-*c*-PNASI as a white powder (4.0 g, 95%). The product was analyzed by NMR spectroscopy to determine the ratio of PNIPAM-*c*-PNASI to be 9:1.

Size distribution measurements of 100 nm silica nanoparticles. A dilute solution of clean 100 nm silica nanoparticles was drop cast onto a clean silicon wafer. After the ethanol evaporated several nanoparticle heights were measured using tapping mode on an Agilent5500 AFM. The results were plot as a histogram to determine the size distribution (Figure 5).

Synthesis of aminated nanoparticles. Silica nanoparticles were aminated in accordance with a literature procedure.[103] Clean and dry silica particles (10 or 100 nm) were added to a solution of toluene (100 mL) containing 3-aminopropyltriethoxysilane (APTES) (11 mL, 47 mmol) and the suspension was refluxed overnight. The reaction mixture was

cooled to room temperature, centrifuged and the solvent decanted to recover the particles. The particles were washed twice with methanol, each time centrifuging the suspended particles and decanting the supernatant solution to recover the particles. After the second methanol wash the particles were dried under vacuum.

Titration of aminated silica nanoparticles. Aminated silica nanoparticles (0.1 g) were placed in 10 mL of 0.01 N HCl and shaken for 3 h. An aliquot of the HCl solution (5 mL) was titrated using 0.01 N NaOH to a phenolphthalein endpoint to calculate the amount of HCl consumed by the amine groups. The 100 nm particles had an amine loading of 0.24 mmol of $–NH_2$ groups/g of SiO_2, while the 10 nm particles had a loading of 0.67 mmol of $–NH_2$ groups /g of SiO_2.

Covalent layer-by-layer assembly of PNIPAM-*c*-PNASI with aminated silica nanoparticles on glass. To functionalize a glass slide, the slide was placed in a U-shaped Teflon holder (Figure 6). The glass slide and Teflon holder were cleaned by 5 min of sonication in hexanes, ethanol, acetone, and 18 MΩ water. The slides in their holder were placed in a piranha solution (3:1, vol/vol 96 % H_2SO_4 / 30 % H_2O_2) at room temperature for 4 h. The slides were then copiously rinsed with 18MΩ water then ethanol. Following the cleaning process, the slides were submerged in ethanol (20 mL) containing APTES (24 µL, 0.1 mmol) and shaken overnight. After this reaction was complete the slides were rinsed with ethanol and dried in a vacuum oven at 120 °C for 3 h. After cooling, the slides were submerged in *N*,*N*-dimethylformamide (DMF) (20 mL) containing PNASI (16 wt %) and shaken overnight. It was then washed 3 times with DMF by shaking approximately 5 min each time. The rinsed slide was submerged in a DMF solution of polyethyleneimine (PEI)

(0.5 wt %) and shaken for 30 min. After washing with DMF three times at 5 min each the slides were submerged in a DMF solution of isopropylamine (2.5 vol %). This three solution cycle involving the initial PNASI treatment, a PEI treatment, and a final isopropylamine treatment was repeated with the PNASI treatment reduced to 30 min. The slide was then submerged in a DMF solution of PNIPAM-*c*-PNASI (approximately 9:1, 20 wt %) and shaken for 30 min. After washing, the slide was placed in a DMF suspension of 100- and 10-nm aminated silica nanoparticles (0.5 wt % each) containing triethylamine (approximately 2.5 vol %) and shaken for 30 min. This 3 step layer-by-layer assembly cycle to form the nanocomposite was completed with a quench of any unreacted NASI groups using a DMF-isopropylamine solution as described in the initial priming steps. This 3 solution process consisting of a PNIPAM-*c*-PNASI treatment, an aminated 10- and 100-nm silica nanoparticle treatments, and a final isopropylamine quench, was repeated 5 times. At the end of the fifth cycle, the slide was treated again with the PNIPAM-*c*-PNASI solution for 30 min. The slide was then allowed to react for 30 min in a suspension containing only 10-nm aminated silica nanoparticles (1.0 wt %) in DMF (20 mL) containing triethylamine (approximately 2.5 vol %). This reaction was followed by shaking the slide for 30 min in the isopropylamine solution. A finishing graft using only the PNIPAM-*c*-PNASI and the isopropylamine solution treatments for 30 min each completed the grafting process. The surface was washed with 18 MΩ water and dried with methanol and N_2 gas.

Functionalization of the glass frits was carried out using a similar procedure. Two frits were placed in a Teflon holder (Figure 7). For frit functionalization, two changes were made to the process used for glass slides: the first reaction time with PNASI at the start of

the assembly was increased to 24 h, and the washing process was changed to include 3-10 min washes with DMF after all polymer reactions.

Contact angle measurements. Using a KSV CAM 200 optical goniometer, contact angles were calculated with the CAM 200 software. The solution was dispensed with an automatic syringe and the water droplet size for static angles on the glass slides was 5 µL. On the glass slides, static angles were measured after a 2 min equilibration time. Advancing contact angles were measured by dispensing the solution at a rate of 1 µL/s. On the glass frits contact angle measurements were only taken for the static contact angle over a 20 min time period or until the solution was completely absorbed into the pores of the surface. The changing contact angle was plotted versus time (Figure 12).

Measuring the reversibility of frit flow rates for water or salt solutions. A functionalized frit was first inserted into a chromatography column to tubing adapter (ACE# 5838-91). The adapter was then attached to a 15-mm i.d. column (ACE#7644-15). Then the frit was washed by letting approximately 2.5 columns of water (ca. 50 mL) pass through the frit. The water washing was followed by washing with approximately 2-cm of methanol (ca. 3.5 mL). After the methanol wash, the frit assembly was dried overnight by flushing purified nitrogen gas through the column and frit setup. After drying the frit approximately 4-cm of water (ca. 7 mL) was allowed to pass through the frit. This was followed by 2-cm of methanol (ca. 3.5 mL). Purified nitrogen gas was then run through the frit for 3 h. After the frit was dried, a ca. 9-mL volume of various salt solutions at various concentrations were added to the column and the volume change was studied until 1-cm (ca. 1.7 mL) of the solution volume has passed through the frit. If the volume change was less than this after 12

h the study was stopped. The remaining salt solution was discarded and the frit assembly was rinsed with approximately 50 mL of 18 MΩ H_2O 4 times before filling the column to 8 cm above the frit top with water. After 3-cm (ca. 5 mL) of water had flowed through the frit the water level was 5 cm above the top of the frit and the flow rate for water was measured over the next 1 cm. The remaining water was removed and 2-cm (ca. 3.5 mL) of methanol was allowed to run through the frit before it was dried for 3 h with nitrogen. The process was then repeated starting with a fresh salt solution with the same concentration and salt (repeatability studies) or with a different salt solution containing a different concentration or a different salt.

Measuring the breakthrough point of sodium sulfate solution. The washing and drying process described above was used for frits 3, 5, and 7. Changes in the process were instigated to measure the breakthrough curves on frits 1 and 8. In this method, the frits were placed in the same chromatography column to tubing adaptors and submerged in cold water which was stirred with an overhead stirrer at approximately 7 °C. After the water was allowed to stir for 3 h, the frits were removed from the water and attached to the glass columns. Approximately 1 column of methanol (ca. 18 mL), was passed through the frit before it was dried by flushing nitrogen through the column and frit for 4 h. The column above the dry frit was then filled with approximately 9-mL of a sodium sulfate solution by filling the solution to 5-cm above the frit top and measuring the flow rate in the manner described above. To clean these frits and proceed to the next measurement, the frit was again removed from the column washed at a low temperature and the rest of the process was repeated. The passive permeability of frits to sodium sulfate concentrations that varied from

1.2 M Na_2SO_4 to 0.1 M to pure 18 MΩ water were then measured with a series of experiments using progressively lower salt concentrations. In the case of frit 8, the measurement of the breakthrough curve using a soaking wash and decreasing salt concentrations was repeated to determine the standard deviation of the flow rates.

IR of a pulverized frit. A functionalized glass frit was pulverized and a sample was used for IR measurements in a KBr pellet.

Raman spectroscopy of a functionalized frit. Raman spectroscopy was performed with a WiTec Alpha300 confocal fluorescence/AFM system on a functionalized frit.

NMR of the polymer from a functionalized surface. A glass frit was sonicated in $CDCl_3$ for 30 min, after which a ^1H NMR spectrum was recorded on the solution.

REFERENCES

(1) Nagel, M. *J. Chem. Educ.* **1980,** *57*, 811-812.

(2) Gil, E. S.; Park, S.-H.; Tien, L. W.; Trimmer, B.; Hudson, S. M.; Kaplan, D. L. *Langmuir* **2010,** *26*, 15614-15624.

(3) Halldorsson, J. A.; Little, S. J.; Diamond, D.; Spinks, G.; Wallace, G. *Langmuir* **2009,** *25*, 11137-11141.

(4) Zhu, D.; Li, X.; Zhang, G.; Zhang, X.; Zhang, X.; Wang, T.; Yang, B. *Langmuir* **2010,** *26*, 14276-14283.

(5) Hernández, R.; Sacristán, J.; Asín, L.; Torres, T. E.; Ibarra, M. R.; Goya, G. F.; Mijangos, C. *J. Phys. Chem. B* **2010,** *114*, 12002-12007.

(6) Li, L.-Y.; He, W.-D.; Li, J.; Zhang, B.-Y.; Pan, T.-T.; Sun, X.-L.; Ding, Z.-L. *Biomacromolecules* **2010,** *11*, 1882-1890.

(7) Sun, S.; Wu, P. *Macromolecules* **2010,** *43*, 9501-9510.

(8) Plunkett, K. N.; Zhu, X.; Moore, J. S.; Leckband, D. E. *Langmuir* **2006,** *22*, 4259-4266.

(9) Myrat, C. D.; Rowlinson, J. S. *Polymer* **1965,** *6*, 645-651.

(10) Zeman, L.; Biros, J.; Delmas, G.; Patterson, D. *J. Phys. Chem.* **1972,** *76*, 1206-1213.

(11) Dimitrov, I.; Trzebicka, B.; Müller, A. H. E.; Dworak, A.; Tsvetanov, C. B. *Prog. Polym. Sci.* **2007,** *32*, 1275-1343.

(12) Popa, A. M.; Angeloni, S.; Bürgi, T.; Hubbell, J. A.; Heinzelmann, H.; Pugin, R. l. *Langmuir* **2010,** *26*, 15356-15365.

(13) Kolaric, B.; Sliwa, M.; Vallée, R. A. L.; Van der Auweraer, M. *Colloids Surf., A* **2009,** *338*, 61-67.

(14) Mao, H.; Li, C.; Zhang, Y.; Bergbreiter, D. E.; Cremer, P. S. *J. Am. Chem. Soc.* **2003,** *125*, 2850-2851.

(15) Panayiotou, M. Synthesis and Characterization of Thermoresponsive Polymers, Hydrogels and Microgels, based on Poly(N-substituted acrylamides). Ph.D. Dissertation, Ecole Polytechnique Federale de Lausanne, 2005.

(16) Etika, K. C.; Jochum, F. D.; Theato, P.; Grunlan, J. C. *J. Am. Chem. Soc.* **2009,** *131*, 13598-13599.

(17) Zhou, Y.; Yan, D.; Dong, W.; Tian, Y. *J. Phys. Chem. B* **2007,** *111*, 1262-1270.

(18) Bergbreiter, D. E.; Fu, H. *J. Polym. Sci., Part A: Polym. Chem.* **2008,** *46*, 186-193.

(19) Kubota, K.; Fujishige, S.; Ando, I. *J. Phys. Chem.* **1990,** *94*, 5154-5158.

(20) Wu, C. *Polymer* **1998,** *39*, 4609-4619.

(21) Zhang, Y.; Guan, Y.; Zhou, S. *Biomacromolecules* **2007,** *8*, 3842-3847.

(22) Elbert, D. L. *Acta Biomater.* **2011,** *7*, 31-56.

(23) Shechter, I.; Ramon, O.; Portnaya, I.; Paz, Y.; Livney, Y. D. *Macromolecules* **2009,** *43*, 480-487.

(24) Nuhn, H.; Klok, H.-A. *Biomacromolecules* **2008,** *9*, 2755-2763.

(25) Terao, K.; Mays, J. W. *Eur. Polym. J.* **2004,** *40*, 1623-1627.

(26) Wu, C.; Wang, X. *Phys. Rev. Lett.* **1998,** *80*, 4092.

(27) Howe, A. M.; Desrousseaux, S.; Lunel, L. S.; Tavacoli, J.; Yow, H. N.; Routh, A. F. *Adv. Colloid Interface Sci.* **2009,** *147-148*, 124-131.

(28) Spevácek, J. *Curr. Opin. Colloid Interface Sci.* **2009,** *14*, 184-191.

(29) Jia, Z.; Chen, H.; Zhu, X.; Yan, D. *J. Am. Chem. Soc.* **2006,** *128*, 8144-8145.

(30) Lee, S. B.; Song, S.-C.; Jin, J.-I.; Sohn, Y. S. *J. Am. Chem. Soc.* **2000,** *122*, 8315-8316.

(31) Gurau, M. C.; Lim, S.-M.; Castellana, E. T.; Albertorio, F.; Kataoka, S.; Cremer, P. S. *J. Am. Chem. Soc.* **2004,** *126*, 10522-10523.

(32) Zhang, Y.; Furyk, S.; Bergbreiter, D. E.; Cremer, P. S. *J. Am. Chem. Soc.* **2005,** *127*, 14505-14510.

(33) Zhang, Y.; Furyk, S.; Sagle, L. B.; Cho, Y.; Bergbreiter, D. E.; Cremer, P. S. *J. Phys. Chem. C* **2007,** *111*, 8916-8924.

(34) Akimoto, J.; Nakayama, M.; Sakai, K.; Okano, T. *Biomacromolecules* **2009,** *10*, 1331-1336.

(35) MacKay, J. A.; Callahan, D. J.; FitzGerald, K. N.; Chilkoti, A. *Biomacromolecules* **2010,** *11*, 2873-2879.

(36) Vermonden, T.; Fedorovich, N. E.; van Geemen, D.; Alblas, J.; van Nostrum, C. F.; Dhert, W. J. A.; Hennink, W. E. *Biomacromolecules* **2008,** *9*, 919-926.

(37) Wang, Y.-C.; Li, Y.; Yang, X.-Z.; Yuan, Y.-Y.; Yan, L.-F.; Wang, J. *Macromolecules* **2009,** *42*, 3026-3032.

(38) Rapoport, N. *Prog. Polym. Sci.* **2007,** *32*, 962-990.

(39) Ball, P. *Nat. Mater.* **2004,** *3*, 210-210.

(40) Liu, Y.-Y.; Zhong, Y.-B.; Nan, J.-K.; Tian, W. *Macromolecules* **2010,** *43*, 10221-10230.

(41) Hoare, T.; Pelton, R. *Langmuir* **2008,** *24*, 1005-1012.

(42) Hamcerencu, M.; Desbrieres, J.; Popa, M.; Riess, G. r. *Biomacromolecules* **2009,** *10*, 1911-1922.

(43) Shi, J.; Alves, N. M.; Mano, J. F. *Macromol. Biosci.* **2006,** *6*, 358-363.

(44) Chun, K. W.; Lee, J. B.; Kim, S. H.; Park, T. G. *Biomaterials* **2005,** *26*, 3319-3326.

(45) Roy, D.; Cambre, J. N.; Sumerlin, B. S. *Prog. Polym. Sci.* **2010,** *35*, 278-301.

(46) Lokuge, I.; Wang, X.; Bohn, P. W. *Langmuir* **2006,** *23*, 305-311.

(47) Hu, J.; Liu, S. *Macromolecules* **2010,** *43*, 8315-8330.

(48) de las Heras Alarcon, C.; Farhan, T.; Osborne, V. L.; Huck, W. T. S.; Alexander, C. *J. Mater. Chem.* **2005,** *15*, 2089-2094.

(49) Lue, S. J.; Hsu, J.-J.; Wei, T.-C. *J. Membr. Sci.* **2008,** *321*, 146-154.

(50) Zelikin, A. N. *ACS Nano* **2010,** *4*, 2494-2509.

(51) Liao, K.-S.; Fu, H.; Wan, A.; Batteas, J. D.; Bergbreiter, D. E. *Langmuir* **2009,** *25*, 26-28.

(52) Chen, T.; Ferris, R.; Zhang, J.; Ducker, R.; Zauscher, S. *Prog. Polym. Sci.* **2010,** *35*, 94-112.

(53) Gras, S. L.; Mahmud, T.; Rosengarten, G.; Mitchell, A.; Kalantar-zadeh, K. *ChemPhysChem* **2007,** *8*, 2036-2050.

(54) Lai, J.-Y.; Lu, P.-L.; Chen, K.-H.; Tabata, Y.; Hsiue, G.-H. *Biomacromolecules* **2006,** *7*, 1836-1844.

(55) Jiang, Y.; Wang, Z.; Yu, X.; Shi, F.; Xu, H.; Zhang, X.; Smet, M.; Dehaen, W. *Langmuir* **2005,** *21*, 1986-1990.

(56) Ernst, O.; Lieske, A.; Holländer, A.; Lankenau, A.; Duschl, C. *Langmuir* **2008,** *24*, 10259-10264.

(57) Amigoni, S.; Taffin de Givenchy, E.; Dufay, M.; Guittard, F. *Langmuir* **2009,** *25*, 11073-11077.

(58) Kidambi, S.; Chan, C.; Lee, I. *Langmuir* **2007,** *24*, 224-230.

(59) Shen, L.; Fu, J.; Fu, K.; Picart, C.; Ji, J. *Langmuir* **2010,** *26*, 16634-16637.

(60) Bergbreiter, D. E.; Liao, K.-S. *Soft Matter* **2009,** *5*, 23-28.

(61) Snyder, D. M. *J. Chem. Educ.* **1989,** *66*, 977-980.

(62) Zeng, G.; Gao, J.; Chen, S.; Chen, H.; Wang, Z.; Zhang, X. *Langmuir* **2007,** *23*, 11631-11636.

(63) Chang, Y. L.; West, M. A.; Fowler, F. W.; Lauher, J. W. *J. Am. Chem. Soc.* **1993,** *115*, 5991-6000.

(64) Kim, D. W.; Blumstein, A.; Kumar, J.; Samuelson, L. A.; Kang, B.; Sung, C. *Chem. Mater.* **2002,** *14*, 3925-3929.

(65) Such, G. K.; Quinn, J. F.; Quinn, A.; Tjipto, E.; Caruso, F. *J. Am. Chem. Soc.* **2006,** *128*, 9318-9319.

(66) Minko, S. *Polym. Rev.* **2006,** *46*, 397-420.

(67) Edmondson, S.; Osborne, V. L.; Huck, W. T. S. *Chem. Soc. Rev.* **2004,** *33*, 14-22.

(68) Zhou, F.; Huck, W. T. S. *Phys. Chem. Chem. Phys.* **2006,** *8*, 3815-3823.

(69) Jordan, R.; Ulman, A.; Kang, J. F.; Rafailovich, M. H.; Sokolov, J. *J. Am. Chem. Soc.* **1999,** *121*, 1016-1022.

(70) Zhao, B.; Zhu, L. *Macromolecules* **2009,** *42*, 9369-9383.

(71) Hirata, I.; Okazaki, M.; Iwata, H. *Polymer* **2004,** *45*, 5569-5578.

(72) Zhang, X.; Wu, T.; Sun, J.; Shen, J. *Colloids Surf., A* **2002,** *198-200*, 439-442.

(73) Kim, D. W.; Kumar, J.; Blumstein, A. *Appl. Clay Sci.* **2005,** *30*, 134-140.

(74) Stockton, W. B.; Rubner, M. F. *Macromolecules* **1997,** *30*, 2717-2725.

(75) Zhai, L.; Cebeci, F. Ç.; Cohen, R. E.; Rubner, M. F. *Nano Lett.* **2004,** *4*, 1349-1353.

(76) Wu, S., *Polymer Interface and Adhesion*. Marcel Dekker Inc.: New York, 1982.

(77) Abbott, N. L.; Whitesides, G. M. *Langmuir* **1994,** *10*, 1493-1497.

(78) Rosslee, C.; Abbott, N. L. *Curr. Opin. Colloid Interface Sci.* **2000,** *5*, 81-87.

(79) Zhao, B.; Haasch, R. T.; MacLaren, S. *Polymer* **2004,** *45*, 7979-7988.

(80) Sun, T.; Wang, G.; Feng, L.; Liu, B.; Ma, Y.; Jiang, L.; Zhu, D. *Angew. Chem., Int. Ed.* **2004,** *43*, 357-360.

(81) Huber, D. L.; Manginell, R. P.; Samara, M. A.; Kim, B.-I.; Bunker, B. C. *Science* **2003,** *301*, 352-354.

(82) Annaka, M.; Yahiro, C.; Nagase, K.; Kikuchi, A.; Okano, T. *Polymer* **2007,** *48*, 5713-5720.

(83) Liu, G.; Zhang, G. *J. Phys. Chem. B* **2004,** *109*, 743-747.

(84) Zhang, G. *Macromolecules* **2004,** *37*, 6553-6557.

(85) Alem, H.; Duwez, A.-S.; Lussis, P.; Lipnik, P.; Jonas, A. M.; Demoustier-Champagne, S. *J. Membr. Sci.* **2008,** *308*, 75-86.

(86) Wandera, D.; Wickramasinghe, S. R.; Husson, S. M. *J. Membr. Sci.* **2010,** *357*, 6-35.

(87) Balogh, D.; Tel-Vered, R.; Riskin, M.; Orbach, R.; Willner, I. *ACS Nano* **2010**, null-null.

(88) Fu, H.; Hong, X.; Wan, A.; Batteas, J. D.; Bergbreiter, D. E. *ACS Appl. Mater. Interfaces* **2010,** *2*, 452-458.

(89) Dong, R.; Lindau, M.; Ober, C. K. *Langmuir* **2009,** *25*, 4774-4779.

(90) Berger, S.; Synytska, A.; Ionov, L.; Eichhorn, K.-J.; Stamm, M. *Macromolecules* **2008,** *41*, 9669-9676.

(91) Xia, F.; Feng, L.; Wang, S.; Sun, T.; Song, W.; Jiang, W.; Jiang, L. *Adv. Mater.* **2006,** *18*, 432-436.

(92) Lim, H. S.; Han, J. T.; Kwak, D.; Jin, M.; Cho, K. *J. Am. Chem. Soc.* **2006,** *128*, 14458-14459.

(93) Blanco-Gomez, G.; Flendrig, L. M.; Cooper, J. M. *Langmuir* **2010,** *26*, 7248-7253.

(94) Wang, W.; Vaughn, M. W. *Scanning* **2008,** *30*, 65-77.

(95) White, L. D.; Tripp, C. P. *J. Colloid Interface Sci.* **2000,** *232*, 400-407.

(96) Ejaz, M.; Tsujii, Y.; Fukuda, T. *Polymer* **2001,** *42*, 6811-6815.

(97) Nyström, D.; Antoni, P.; Malmström, E.; Johansson, M.; Whittaker, M.; Hult, A. *Macromol. Rapid Commun.* **2005,** *26*, 524-528.

(98) Liu, X.; Ye, Q.; Yu, B.; Liang, Y.; Liu, W.; Zhou, F. *Langmuir* **2010,** *26*, 12377-12382.

(99) Wolansky, G.; Marmur, A. *Colloids Surf., A* **1999,** *156*, 381-388.

(100) Golden, A. L.; Battrell, C. F.; Pennell, S.; Hoffman, A. S.; J. Lai, J.; Stayton, P. S. *Bioconjugate Chem.* **2010,** *21*, 1820-1826.

(101) Schepelina, O.; Zharov, I. *Langmuir* **2007,** *23*, 12704-12709.

(102) Zhilova, S. B.; Karov, Z. G.; El'mesova, R. M. *Russ. J. Inorg. Chem.* **2008,** *53*, 628-635.

(103) Bergbreiter, D. E.; Simanek, E. E.; Owsik, I. *J. Polym. Sci., Part A: Polym. Chem.* **2005,** *43*, 4654-4665.

VITA

Name:	Ainsley LaRue Allen
Address:	Department of Chemistry, Texas A&M University PO Box 30012, College Station, TX 77842-3012
Email Address:	c09ainsley.allen@gmail.com
Education:	B.S., Chemistry, United States Air Force Academy, 2009 M.S., Chemistry, Texas A&M University, 2011